Chapter 2
Equations Governing Flow and Transport in Porous Media

K. Muralidhar

In the simplest situation of a large bed of small rigid spheres of uniform diameter, flow in the pore space can be represented by Darcy's law [1]. As discussed in Chap. 1, this relationship, stated at the scale of the representative elementary volume (REV), arises from volume-averaging Navier–Stokes equations at the low Reynolds number limit in a repeating geometry [2, 3]. Historically, Darcy's law was proposed as an empirical relationship on the basis of laboratory experiments while the theoretical basis was developed in later years. In this respect, the mass, momentum, and energy equations in a porous medium are posed as mathematical models rather than natural laws. This spirit of empirical–theoretical formulation of flow and transport in porous media has pervaded analysis and will be followed in the rest of the chapter.

With burgeoning applications in porous media, a wide variety of possibilities may be realized during flow and transport. While single and multiphase flows in porous media are discussed in the following sections, several other specialized topics such as radiative transport and solid–fluid phase change have not been covered [4–6]. The discussion here is restricted to devices and processes in which one or more fluids pass through the porous region, exchanging energy and mass with the solid phase.

2.1 Darcy's Law

Originally stated for a bed of spheres, Darcy's law for fluid flow in the pore space is given by the relationship

$$\mathbf{u} = -\frac{K}{\mu}\nabla p \tag{2.1}$$

Here, $\mathbf{u}$ is the fluid velocity obtained as an average over the REV, and p is fluid pressure at the pore scale. The symbol K represents the medium permeability, and

M.K. Das et al., *Modeling Transport Phenomena in Porous Media with Applications*, Mechanical Engineering Series,
https://doi.org/10.1007/978-3-319-69866-3_2

μ is the dynamic viscosity of the fluid. The porous medium is taken to be *saturated* with the fluid of interest in the sense that fluid–fluid interfaces do not form, and a single fluid prevails in the pore space. Let d_p be the particle size and U, a velocity scale. Equation 2.1 has been found to be applicable for Reynolds number of up to unity, namely [1–3, 6, 7]

$$\mathrm{Re} = \frac{\rho U d_p}{\mu} < 1$$

The permeability of a porous medium is a property that depends on the pore size and the pore structure. The fact that permeability may vary from one geometry to another makes the applicability of Eq. 2.1 quite restrictive. On the other hand, dimensional analysis shows permeability to be a function of porosity ε and particle diameter d_p, each representing the pore geometry and pore size, respectively. The Carman–Kozeny relationship connects these quantities empirically but with dimensional correctness as [2, 8, 9]

$$K = \frac{d_p^2 \varepsilon^3}{180(1-\varepsilon)^2} \tag{2.2}$$

With the particle diameter expressed in meters, permeability has dimensions of m^2. In applications, one can expect to have a length scale for the device itself, say L, and the ratio defined as

$$Da = \frac{K}{L^2} \tag{2.3}$$

is called the Darcy number. In many applications, the particle diameter is of the order of a fraction of a millimeter while the device length scale is around a meter or beyond. Naturally, Darcy numbers of the order of 10^{-6} and smaller and quite common. Larger Darcy numbers will indicate larger particle diameter and pore size. The resulting Reynolds number will be greater than unity leading to a violation of Darcy's law. Hence, Eq. 2.1 can be properly stated as being applicable in the limit of $Da << 1, \mathrm{Re} < 1$.

The Carman–Kozeny relationship for permeability has limited applicability. Even for a regular bed of spheres, the numerical factor shows a spread over 150–180. It has the advantage of representing the flow space in terms of porosity while the flow size is referred to the particle diameter. These small-scale features are then projected on to the size of the REV. In more complex systems such as meshes and an array of cylinders that are assumed to behave like porous media, an explicit permeability–porosity relationship may not exist. Equation 2.1 must then be used to determine permeability from a calibration experiment where pressure drop and velocity are individually measured [10].

Darcy's law (Eq. 2.1) is remarkably similar to Fourier's law of heat conduction where the heat flux and temperature gradient are connected via thermal

conductivity. Heat transfer across a finite temperature difference is thermodynamically irreversible with a local dissipation rate proportional to the product of temperature gradient and heat flux. Analogously, flow through porous media is irreversible, and the power required to sustain flow is proportional to the product of velocity and pressure gradient. The power thus supplied is internally dissipated as thermal energy through the action of viscosity.

Darcy's law is most appropriately used to determine fluid velocity and the flow rate, when the pressure gradient is known. For example, flow in a tube filled with a porous medium will experience a pressure drop of $p_2 - p_1 = \Delta p$ over a length L between points 1 and 2. The average fluid velocity in the tube along its axis can now be calculated as

$$u = -\frac{K}{\mu}\left(\frac{\Delta p}{L}\right) = \frac{K}{\mu}\frac{p_1 - p_2}{L}$$

Volume flow rate is obtained as a product of velocity and the cross-sectional area. The power consumed to sustain flow is the product of pressure drop and volume flow rate.

In a multidimensional flow field, the local pressure gradient is also an unknown. Here, Darcy's law is viewed as a momentum equation wherein pressure gradient balances viscous forces at the fluid–particle boundary. Other contributions such as body forces, inertia, and unsteadiness are set to zero. The momentum equation is then to be supplemented by the mass balance equation. Assuming flow to be incompressible, mass balance equation at the scale of the REV is given as [4–9, 11]:

$$\nabla \cdot \mathbf{u} = 0 \tag{2.4}$$

Equations (2.1) and (2.4) can be jointly used to obtain the flow and pressure distribution in the porous medium.

To a first approximation, Darcy's law is applicable without change during flow transients as well. The justification here is that the characteristic length scale related to the duration of the transient, namely d_p, the particle diameter, is small. Consequently, the timescale

$$\tau = \frac{d_p}{U}$$

is also a small quantity. In applications, the timescale over which changes in pressure and velocity take place are usually much larger. For conditions where flow or pressure is driven in time, Darcy's law (Eq. 2.1) is now taken to be applicable for each time instant.

Between velocity and pressure, velocity can be eliminated using the mass balance equation, yielding a single equation for pressure, namely

$$\nabla^2 p = 0 \tag{2.5}$$

The pressure equation can be solved along with suitable boundary conditions. Combined with Eq. 2.1, the velocity field can be mapped in the porous region.

2.1.1 Cartesian and Cylindrical Coordinate Systems

Equation 2.5 is in coordinate-free form; specific forms of the pressure equation in Cartesian and cylindrical coordinate systems are given as follows:

$$\begin{aligned} &\text{Cartesian} \quad \frac{\partial^2 p}{\partial x^2} + \frac{\partial^2 p}{\partial y^2} + \frac{\partial^2 p}{\partial z^2} = 0 \\ &\text{Cylindrical} \quad \frac{\partial^2 p}{\partial r^2} + \frac{1}{r}\frac{\partial p}{\partial r} + \frac{1}{r^2}\frac{\partial^2 p}{\partial \theta^2} + \frac{\partial^2 p}{\partial z^2} = 0 \end{aligned} \tag{2.6}$$

The velocity components are determined using Eq. 2.1 as:

$$\begin{aligned} &\text{Cartesian} \quad u = -\frac{K}{\mu}\frac{\partial p}{\partial x} \quad v = -\frac{K}{\mu}\frac{\partial p}{\partial y} \quad w = -\frac{K}{\mu}\frac{\partial p}{\partial z} \\ &\text{Cylindrical} \quad u^r = -\frac{K}{\mu}\frac{\partial p}{\partial r} \quad u^\theta = -\frac{1}{r}\frac{K}{\mu}\frac{\partial p}{\partial \theta} \quad u^z = -\frac{K}{\mu}\frac{\partial p}{\partial z} \end{aligned} \tag{2.7}$$

Equations 2.5–2.6 can be solved by the tools of classical analysis [12–14], for example, separation of variables in finite domains of regular shape and transform techniques in semi-infinite geometries. They require prescription of boundary conditions over the entire boundary in one of the following standard forms:

$$\begin{aligned} &\text{Dirichlet: } p(x,y,z) \text{specified} \\ &\text{Neumann: } \frac{\partial p}{\partial n} \text{specified} \\ &\text{Robin: } ap(x,y,z) + b\frac{\partial p}{\partial n} \text{ specified (constants } a \text{ and } b) \end{aligned} \tag{2.8}$$

For example, at an injection or fluid production point, pressure is specified. On a no-flow, impermeable boundary, the normal derivative of pressure is zero. The third category of boundary condition is also possible. The specified quantity can be zero, a constant, or a function of time.

Some porous media problems can be formulated with volumetric sources (of mass) distributed as $Q(\mathbf{x})$ (units of m^3/s per m^3 volume of REV) for which the mass balance equation is written as

$$\nabla \cdot \mathbf{u} = Q$$

Combined with Darcy's law, the pressure equation takes on the form

$$\nabla^2 p + \frac{\mu}{K} Q = 0$$

The boundary conditions continue to be given by Eq. 2.8.

Since the pressure gradient along a solid wall is nonzero, the tangential component of wall velocity is nonzero and the no-slip condition does not hold. For an impermeable wall, the normal derivative of pressure is zero, and hence, the normal velocity is also zero. The inapplicability of the no-slip velocity condition is peculiar to the Darcy formulation of flow in porous media. The non-Darcy system of equations (Sect. 2.4) permits the no-slip condition and is more realistic.

For a clear fluid medium lying adjacent to a porous medium, the boundary conditions for Navier–Stokes equations are modified to account for slip at the interface. In place of the no-slip condition, the following Beavers–Sparrow condition [9] is utilized:

$$\frac{\partial u_f}{\partial y} = \frac{\alpha_{BJ}}{\sqrt{K}} (u_f - u_{PM})$$

Here, suffix '*f*' refers to the clear fluid medium, *PM* is the porous medium, and α_{BJ} is an empirical (Beavers–Joseph) parameter. The Dirichlet boundary condition for velocity is now replaced by a Neumann condition. It can be expected that the normal velocity component will remain continuous across the clear–porous interface. The governing equations in the porous medium and the clear fluid are thus coupled at their interface.

2.1.2 Inhomogeneous Media

Here, the pore space dimensions may vary from one location to another. If an average pore dimension can be identified at the scale of the REV, one can define a permeability function $K(\mathbf{x})$ and the corresponding form of Darcy's law

$$\mathbf{u} = -\frac{K(\mathbf{x})}{\mu} \nabla p \tag{2.9}$$

Combining with the mass balance equation, Eq. 2.9 can be expressed in terms of pressure as

$$\nabla \cdot \{K(\mathbf{x})\nabla p\} = 0 \tag{2.10}$$

The pressure equation is solved along with the Dirichlet, Neumann, or Robin boundary conditions described by Eq. 2.8. Equation 2.10 expressed in Cartesian coordinates is of the form

$$\frac{\partial}{\partial x}\left[K(x,y,z)\frac{\partial p}{\partial x}\right] + \frac{\partial}{\partial y}\left[K(x,y,z)\frac{\partial p}{\partial y}\right] + \frac{\partial}{\partial z}\left[K(x,y,z)\frac{\partial p}{\partial z}\right] = 0$$

2.1.3 Anisotropic Media

Darcy's law (Eq. 2.1) can be expressed in index notation as

$$u_i = -K\frac{\partial p}{\partial x_i} \tag{2.11}$$

Here, permeability is a scalar function that is a constant or a prescribed function of position, as in Eq. 2.9. Equation 2.11 also admits tensor forms of permeability wherein permeability is a Cartesian second-order tensor, namely

$$u_i = -K_{ij}\frac{\partial p}{\partial x_j} \tag{2.12}$$

Equation 2.12 expands in a Cartesian coordinate system as

$$\begin{aligned} u &= -K_{11}\frac{\partial p}{\partial x} - K_{12}\frac{\partial p}{\partial y} - K_{13}\frac{\partial p}{\partial z} \\ v &= -K_{21}\frac{\partial p}{\partial x} - K_{22}\frac{\partial p}{\partial y} - K_{23}\frac{\partial p}{\partial z} \\ w &= -K_{31}\frac{\partial p}{\partial x} - K_{32}\frac{\partial p}{\partial y} - K_{33}\frac{\partial p}{\partial z} \end{aligned} \tag{2.13}$$

Here, K_{ij} is a permeability tensor and has nine components, with indices 'i' and 'j' running over 1…3. These respectively refer to the Cartesian coordinate directions x, y, and z. Combining with the continuity equation, Eq. 2.13 can be cast in a form suitable for pressure calculation as [15]

$$\begin{aligned} &\frac{\partial}{\partial x}\left[K_{11}\frac{\partial p}{\partial x} + K_{12}\frac{\partial p}{\partial y} + K_{13}\frac{\partial p}{\partial z}\right] + \frac{\partial}{\partial y}\left[K_{21}\frac{\partial p}{\partial x} + K_{22}\frac{\partial p}{\partial y} + K_{23}\frac{\partial p}{\partial z}\right] \\ &\quad + \frac{\partial}{\partial z}\left[K_{31}\frac{\partial p}{\partial x} + K_{32}\frac{\partial p}{\partial y} + K_{33}\frac{\partial p}{\partial z}\right] = 0 \end{aligned} \tag{2.14}$$

In homogeneous media, the permeability tensor is symmetric, and the nine components reduce to six. In isotropic and homogeneous media, the nine components of the permeability tensor reduce to one, making permeability a scalar quantity. It is worth repeating here that Darcy's law as given by Eq. 2.1 is applicable for a homogeneous and isotropic medium, characterized by a scalar permeability.

In an orthotropic medium, the off-diagonal components of permeability are zero while the principal components of permeability are nonzero and distinct. Here

$$K_{ij} = \begin{bmatrix} K_{11} & 0 & 0 \\ 0 & K_{22} & 0 \\ 0 & 0 & K_{33} \end{bmatrix}$$

The pressure equation can now be derived as

$$\frac{\partial}{\partial x}\left(K_{11}\frac{\partial p}{\partial x}\right) + \frac{\partial}{\partial y}\left(K_{22}\frac{\partial p}{\partial y}\right) + \frac{\partial}{\partial z}\left(K_{33}\frac{\partial p}{\partial z}\right) = 0 \tag{2.15}$$

The permeability components K_{ii} can be functions of position or take on purely constant values. For a homogeneous and isotropic medium,

$$K_{11} = K_{22} = K_{33} = K$$

For anisotropic media, one can identify principal directions with respect to which the off-diagonal components of permeability are zero. The Cartesian coordinate system can then be aligned with the principal directions of the porous medium being studied, leading to some simplification in the governing equations.

2.1.4 Compressible Flow

For a start, think of a porous medium whose pore space does not alter with pressure, so that it is characterized by a constant porosity. In certain circumstances, the fluid filling the pore space may have to be treated as compressible. The mass balance equation for a compressible fluid in a fixed pore space is now expressed as

$$\varepsilon\frac{\partial \rho}{\partial t} + \nabla \cdot \rho\mathbf{u} = 0 \tag{2.16}$$

Here, ρ is fluid density, ε is porosity, and $\mathbf{u}$ is the REV-averaged fluid velocity. With mass sources, the right-hand side is replaced by $\rho Q(\mathbf{x})$. Eq. 2.16 follows the mass balance equation of a compressible fluid of homogeneous fluid-filled porous media, except that the first term includes porosity. This correction arises from the fact that the amount of fluid contained in the REV is a fraction of the volume of REV, as defined by the porosity.

If the flow rates are small enough for the pore-scale Reynolds number to be less than unity, Stokes equations will hold in the fluid phase, and its integrated form at the scale of the REV, namely Darcy's law (Eq. 2.1), can once again be used as a momentum equation. Hence, working with a homogeneous and isotropic medium, velocity and pressure are connected as

$$\mathbf{u} = -\frac{K}{\mu}\nabla p$$

The system of equations can be closed when an equation of state relating density and pressure is prescribed. For gases, changes in density will be accompanied by those in pressure and temperature. Accordingly, an energy equation is added to the system of equations governing compressible flow of gas in a porous medium. For a liquid, density may be connected to pressure through compressibility S as

$$S = \frac{1}{\rho}\frac{\partial \rho}{\partial p}$$

Here, S is a positive quantity (units of $(\mathrm{N/m^2})^{-1}$) and is a constant over a range of fluid pressures. Combining the unsteady mass balance equation with Darcy's law, we get

$$S\rho\varepsilon\frac{\partial p}{\partial t} = \nabla \cdot \left(\rho\frac{K}{\mu}\nabla p\right)$$

A simplified form of the pressure equation that is adequate for mildly compressible fluids ($\rho \sim$ constant) can be derived by canceling density on both sides. It reads

$$\frac{\partial p}{\partial t} = \frac{K}{\mu S\varepsilon}\nabla^2 p \tag{2.17}$$

If the porous medium is also compressible, S can be interpreted as the combined compressibility of the medium and the fluid within. Equation 2.17 shows that the role of compressibility is to sustain flow transients in a porous medium.

The unsteady pressure equation for a compressible liquid in an incompressible porous medium has a form analogous to the diffusion equation of heat transfer. Analytical solutions developed in specialized texts related to conduction heat transfer can be extended to the present context [14].

Compressibility of the fluid is important for gaseous media. It is also important when liquids are pumped at high pressures through a porous reservoir. For small pore dimensions, permeability (and hence, Darcy number) is small, pressure drop is large, and compressibility will once again be relevant.

If the porous medium carried gas, the compressibility relationship emerges (to a first approximation) via the ideal gas law

$$\frac{p}{\rho} = RT$$

For near-isothermal conditions, we may write $\rho = Cp$ for the ideal gas law leading to the nonlinear governing equation

$$\frac{\partial p}{\partial t} = \nabla \cdot \left(\frac{K}{\mu \varepsilon} \nabla p^2 \right) \tag{2.18}$$

For steady state, Eq. 2.18 is linear in the new variable—square of pressure. For constant properties, Eq. 2.18 simplifies to

$$\nabla \cdot \nabla p^2 = 0$$

2.1.5 *Effect of Gravity*

In large-scale reservoirs, gravity forces become relevant and alter the flow field. Gravity-related corrections will appear in the momentum equation, namely Darcy's law in the form

$$u = -\frac{K}{\mu}(\nabla p + \rho g) = -\frac{K}{\mu}(\nabla \tilde{p}) \tag{2.19}$$

Here $\tilde{p} = p + \rho g z$. Symbol z stands for the vertical direction opposed to the direction of gravity. The augmented pressure variable can be interpreted as a gravity-modified pressure. Equations derived earlier carry over unchanged with p replaced by $\tilde{p}$, when gravitational effects are to be accounted for.

2.2 Brinkman-Corrected Darcy's Law

Consider the simplest layout of flow in a parallel plate channel of length L and opening $2H$, filled with homogeneous isotropic porous media of permeability K, driven by an overall pressure difference. The governing equation for pressure reduces to

$$\frac{d^2 p}{dx^2} = 0$$

The pressure variation is thus linear in the flow direction; using Darcy's law, the velocity components are evaluated as

$$u = -\frac{K}{\mu}\frac{p_2 - p_1}{L}; \quad v = 0$$

The velocity components predicted by Darcy's law are seen here to be independent of the axial coordinate and hence, *fully developed*. When the pressure difference changes with time, the x-component of velocity will change instantaneously, without any time lag. These results are not unexpected because the characteristic length scale that determines transient duration as well as the flow development is the pore diameter, which is a small quantity, relative to H and L.

A second consequence of a constant velocity component is that it is spatially uniform in the cross-sectional y-direction, including the wall. This solution violates the no-slip condition between a fluid and a solid boundary commonly seen in continuum flow applications. The interpretation here is that porous media lead to extremely thin wall boundary layers. The spatially uniform velocity solution is then applicable in an experiment over most of the channel width. Based on dimensional reasoning, one can expect the boundary-layer thickness to scale with $\sqrt{K}$, and so with the square root of Darcy number $\sqrt{Da} = \sqrt{K}/H$, where H is the channel half-width. Thus, the constant velocity solution is expected to be realized in dense, low permeability porous media. Here, pressure drop arises mainly from skin friction within the body of the porous medium, unlike homogeneous fluids where the origin of pressure drop is skin friction at the solid walls.

The uniform velocity solution is expected to fail in moderate and high permeability porous regions confined in a channel or a tube. An additional factor that needs consideration is the variation of permeability of a porous region near a solid wall. As shown in Fig. 2.1, porosity near a wall is greater in comparison to the bulk, leading to higher permeability. The wall boundary layers are thickened, and the entire velocity profile can now be obtained only after accounting for the no-slip condition.

A useful framework for introducing the no-slip condition in Darcy's law is available through the Brinkman's approximation which introduces a viscous shear stress term in Darcy's law. The Brinkman-corrected Darcy's law is written as

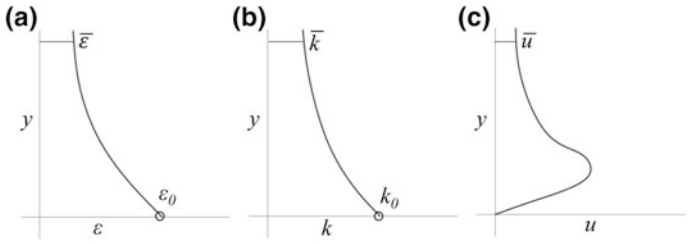

Fig. 2.1 **a–b** Wall porosity and permeability variation in a channel; **c** schematic drawing of velocity variation in the near-wall region; peak porosity and permeability are indicated as ε_0 and K_0 respectively

$$-\nabla p - \frac{\mu}{K}u + \frac{\tilde{\mu}}{\varepsilon}\nabla^2 \mathbf{u} = 0 \tag{2.20}$$

Comparing with Eq. 2.1, the correction is seen in the third term involving an effective viscosity $\tilde{\mu}$. Given the overall uncertainty in model parameters such as K and ε, the effective viscosity is approximated as the fluid viscosity itself [8, 9].

Since Eq. 2.20 is a second-order partial differential equation in velocity, the no-slip condition can now be conveniently introduced at the walls. A sample solution of velocity distribution is sketched in Fig. 2.1. The overall pressure drop will arise from shear stresses at the liquid–particle interface of the porous region as well as stresses at the liquid–channel boundary that enforce the no-slip condition. It may be noted in Fig. 2.1 that the near-wall velocity variation has a local maximum arising from larger porosity and permeability, a phenomenon called *channeling*. It refers to preferential flow in the near-wall region owing a larger pore scale in comparison to the bulk of the porous medium.

2.3 Forschheimer-Extended Darcy's Law

Darcy's law requires correction when the particle-diameter-based Reynolds number exceeds unity. Such a flow field is commonly encountered in high porosity systems where the fluid velocities are high. In gas flows, viscosity is low, and Reynolds numbers can once again exceed unity.

The immediate consequence of increasing Reynolds number is that form drag experienced by the particles of the solid phase becomes larger in relation to viscous drag. In the limiting case of high Reynolds numbers, form drag can be substantially larger than viscous drag. Figure 2.2 shows the variation of drag coefficient C_D of a sphere as a function of Reynolds number Re_d. With D as total drag,

$$C_D = \frac{D}{\frac{1}{2}\rho u^2 A_p} \quad \text{and } \mathrm{Re}_d = \frac{\rho u d}{\mu}$$

Here, ρ is fluid density and A_p is a reference area, usually chosen as the projected area of the object normal to the flow direction. For a sphere of diameter d,

$$A_p = \pi d^2$$

For small Reynolds numbers, drag coefficient decreases with Re_d, giving rise to the following scaling relation:

$C_D = \dfrac{D}{\frac{1}{2}\rho u^2 A_p} = \dfrac{A}{\mathrm{Re}_d}$. Hence, drag varies as $D = \text{constant} \times u$

For larger Reynolds numbers ($20 < \mathrm{Re}_d < 10{,}000$), Fig. 2.2 shows near constancy of the drag coefficient. Hence

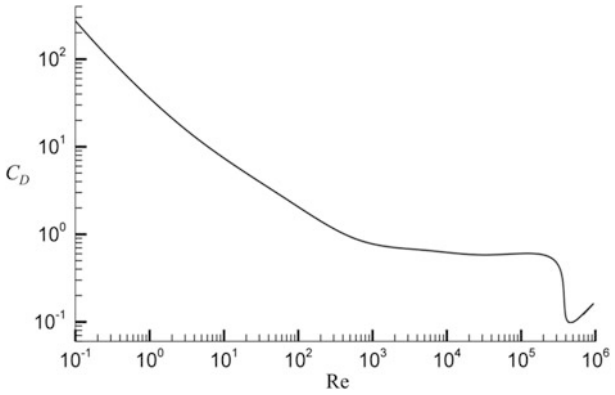

Fig. 2.2 Variation of drag coefficient with Reynolds number for a sphere placed in uniform approach flow

$$C_D = \frac{D}{\frac{1}{2}\rho u^2 A_p} = \text{constant} \sim 1; \quad D = \text{constant} \times u^2$$

Combining the two limits, one can write the following expression for drag experienced by a particle of the porous medium:

$$D = au + bu^2$$

The square-law dependence arises from an adverse pressure gradient and flow separation at the surface the sphere. The quadratic trend realized for a single sphere can be extended to a porous medium comprising a bed of spheres. Experiments indeed show that a porous medium made up of small particles will show drag scaling linearly with velocity at a low Reynolds number and square of velocity for $\text{Re} \gg 1$. The low Reynolds number limit of drag proportional to velocity translates as Darcy's law (Eq. 2.1). An extended form of Darcy's law valid for a wider range Reynolds numbers can be written analogously to drag coefficient as

$$\frac{\Delta p}{L} = -\frac{\mu}{K}u - \frac{\rho F}{\sqrt{K}}u^2$$

The symbol Δp represents pressure drop and is negative with respect to the flow direction. Here, F is a parameter to be determined from experiments. For a bed of uniform-diameter rigid spheres, the following correlation has been reported in the literature [5, 8, 9]:

$$F = \frac{1.8}{(180\varepsilon^5)^{0.5}}\varepsilon$$

In applications, it will have to be experimentally determined from calibration experiments; see Chap. 6 for an example. The square-law correction of Darcy's law is called the Forschheimer term, F being the Forschheimer constant. Darcy's law generalized to accommodate a wider range of Reynolds numbers is expressed as

$$-\nabla p - \frac{\mu}{K}\mathbf{u} - \frac{\rho F}{\sqrt{K}}\mathbf{u}|\mathbf{u}| = 0 \tag{2.21}$$

The modulus of velocity ensures that the formulation is correct for positive as well as negative flow directions.

The Brinkman and Forschheimer-corrected Darcy's law is written as

$$-\nabla p - \frac{\mu}{K}\mathbf{u} - \frac{\rho F}{\sqrt{K}}\mathbf{u}|\mathbf{u}| + \frac{\mu}{\varepsilon}\nabla^2\mathbf{u} = 0 \tag{2.22}$$

Equation 2.22 is a form of a momentum equation in which a balance of fluid pressure, viscous forces at the fluid–particle boundary, viscous forces within the fluid medium, generally arising at the confining walls, and form drag is attained at the scale of the REV.

2.4 Non-darcy Model of Flow

Equation 2.22 extends Darcy's law by including a variety of external forces. Indeed, this approach can be used to bring in additional forces arising from, for example, buoyancy and electromagnetism. Equation 2.22 requires the sum of all external forces to be zero, a condition applicable only for non-accelerating flow fields. The expression for fluid acceleration a in a Lagrangian frame of reference can be written as

$$\mathbf{a} = \frac{1}{\varepsilon}\frac{d\mathbf{u}}{dt}$$

Here, the symbol $\mathbf{u}$ continues to represent the REV-averaged velocity, with $\mathbf{u}/\varepsilon$ being the local fluid velocity vector. Hence, acceleration referred here is that of the fluid alone, while the solid phase is stationary.

It is useful to employ the Eulerian representation of acceleration [11]

$$\mathbf{a} = \frac{1}{\varepsilon}\frac{d\mathbf{u}}{dt} = \frac{1}{\varepsilon}\left(\frac{\partial \mathbf{u}}{\partial t} + \frac{1}{\varepsilon}\mathbf{u}\cdot\nabla\mathbf{u}\right)$$

Temporal and spatial acceleration terms are now explicitly written out. Equating the sum of all external forces to mass $\times$ acceleration, Eq. 2.22 can be generalized to the form

$$\frac{\rho}{\varepsilon}\frac{d\mathbf{u}}{dt} = -\nabla p - \frac{\mu}{K}\mathbf{u} - \frac{\rho F}{\sqrt{K}}\mathbf{u}|\mathbf{u}| + \frac{\mu}{\varepsilon}\nabla^2\mathbf{u}$$

Here, ρ is fluid density. Hence

$$\frac{\rho}{\varepsilon}\left(\frac{\partial \mathbf{u}}{\partial t} + \frac{1}{\varepsilon}\mathbf{u}\cdot\nabla\mathbf{u}\right) = -\nabla p - \frac{\mu}{K}\mathbf{u} - \frac{\rho F}{\sqrt{K}}\mathbf{u}|\mathbf{u}| + \frac{\mu}{\varepsilon}\nabla^2\mathbf{u} \tag{2.23}$$

Equation 2.23 is called the *non-Darcy model* of fluid flow in a porous medium and is applicable over a range of Reynolds numbers [5, 8, 9, 16–18].

When gravity effects are important, pressure can be replaced by the effective pressure as in Eq. 2.19. This approach is applicable for all body force fields χ that are expressible as a gradient of a scalar potential ($\chi = -\nabla\phi$). Then, $\tilde{p} = p + \phi$.

Equation 2.23 can be seen from other viewpoints as discussed in the following remarks.

i. The non-Darcy model represents flow in a homogenized porous medium where the building block is the representative elementary volume (REV). Local averaging yields new parameters such as $\varepsilon, K,$ and F apart from fluid properties ρ and μ.
ii. The fluid phase in the pores of the physical domain pass through a tortuous path may suffer local adverse pressure gradients and flow separation. These classify as acceleration but are submerged in the volume-averaging step over the REV, leading to the Forschheimer correction. The acceleration terms of Eq. 2.23 will be explicitly nonzero when inflow velocities change with time, the macroscopic flow passage is of variable area, and over geometries such as a cylinder buried in a porous formation.
iii. The basic unknowns of the non-Darcy model are the velocity components that are derivable from the momentum equations and pressure. The latter is obtained from the mass conservation equation, which for an incompressible, fluid saturated porous medium is given by Eq. 2.4 as

$$\nabla\cdot\mathbf{u} = 0$$

iv. Uncertainties in the specification of the effective viscosity (approximated often as the fluid viscosity) and the correlations for K and F contribute to the overall model uncertainty. In turn, these quantities are to be found from benchmark experiments where the flow distribution and pressure drop can be easily measured. The overall approach of extracting the constants of proportionality from experiments falls in the domain of *parameter estimation*.
v. For a homogeneous fluid, $\varepsilon \to 1$ and $K \to \infty$ and Eq. 2.23 reduces to the classical Navier–Stokes equations [11]

$$\rho\left(\frac{\partial \mathbf{u}}{\partial t}+\mathbf{u}\cdot\nabla\mathbf{u}\right)=-\nabla p+\mu\nabla^2\mathbf{u}$$

vi. For definiteness, consider flow in a parallel plate channel filled with a homogeneous and isotropic porous medium. Following the initial and boundary conditions employed in the context of fluid flow problems, those for the non-Darcy model can be stated as follows.

prescribed or quiescent initial flow field,
prescribed inlet velocity distribution,
no-slip and impermeability conditions for velocity at solid surfaces,
fully developed flow at the exit plane, and
pressure specified at one point on the exit plane.

vii. The non-Darcy model shares several mathematical properties with the Navier–Stokes equations. For example, both are second-order nonlinear partial differential equations in space and first order in time. Hence, semi-analytical and numerical methods such as computational fluid dynamics (CFD) applicable for the Navier–Stokes equations can be carried forward to flow in porous media [19].

viii. Equation 2.23 is in coordinate-free form and can be expanded in a coordinate system of interest by using the correct form of the derivative operators. Let (u, v, w) represent the Cartesian components of velocity in the (x, y, z) coordinate system. The three-dimensional unsteady form of the non-Darcy equations can be expressed as follows:

$$\frac{\partial u}{\partial x}+\frac{\partial v}{\partial y}+\frac{\partial w}{\partial z}=0 \tag{2.24}$$

$$\begin{aligned}
&\frac{\rho}{\varepsilon}\left(\frac{\partial u}{\partial t}+\frac{1}{\varepsilon}\left(u\frac{\partial u}{\partial x}+v\frac{\partial u}{\partial y}+w\frac{\partial u}{\partial z}\right)\right)=-\frac{\partial p}{\partial x}-\frac{\mu}{K}u\\
&\quad-\frac{\rho F}{\sqrt{K}}u\sqrt{u^2+v^2+w^2}+\mu\left(\frac{\partial^2 u}{\partial x^2}+\frac{\partial^2 u}{\partial y^2}+\frac{\partial^2 u}{\partial z^2}\right)\\
&\frac{\rho}{\varepsilon}\left(\frac{\partial v}{\partial t}+\frac{1}{\varepsilon}\left(u\frac{\partial v}{\partial x}+v\frac{\partial v}{\partial y}+w\frac{\partial v}{\partial z}\right)\right)=-\frac{\partial p}{\partial y}-\frac{\mu}{K}v\\
&\quad-\frac{\rho F}{\sqrt{K}}v\sqrt{u^2+v^2+w^2}+\mu\left(\frac{\partial^2 v}{\partial x^2}+\frac{\partial^2 v}{\partial y^2}+\frac{\partial^2 v}{\partial z^2}\right)\\
&\frac{\rho}{\varepsilon}\left(\frac{\partial w}{\partial t}+\frac{1}{\varepsilon}\left(u\frac{\partial w}{\partial x}+v\frac{\partial w}{\partial y}+w\frac{\partial w}{\partial z}\right)\right)=-\frac{\partial p}{\partial z}-\frac{\mu}{K}w\\
&\quad-\frac{\rho F}{\sqrt{K}}w\sqrt{u^2+v^2+w^2}+\mu\left(\frac{\partial^2 w}{\partial x^2}+\frac{\partial^2 w}{\partial y^2}+\frac{\partial^2 w}{\partial z^2}\right)
\end{aligned} \tag{2.25}$$

ix. Once the local flow field and pressure distribution are solved for quantities such as flow rate and surface forces on a global scale can be obtained by suitably integrating the local distributions of velocity, pressure, and shear stresses. Equations 2.24 and 2.25 are coupled in terms of velocity components and pressure. Coupling, nonlinearity, and the overall complexity of the governing equations make analysis of the flow field quite daunting.

2.4.1 Non-dimensionalization

Let L be a macroscopic length scale and U a velocity scale chosen for the device or the apparatus of interest. For homogeneous fluid flow, the scaling law for dimensionless quantities leads to the definition of the Reynolds number

$$\mathrm{Re} = \frac{\rho UL}{\mu}$$

In dimensionless form, velocity is interpreted as the scaled variable u/U and pressure as $(p - p_{\mathrm{ref}})/\rho U^2$, while the independent variables are scaled as $x \rightarrow x/L$ and $t \rightarrow Ut/L$. During the process of scale analysis, the continuity equation remains unchanged.

The dimensionless Navier–Stokes equations written in coordinate-free form can be readily derived as [11]

$$\left(\frac{\partial \mathbf{u}}{\partial t} + \mathbf{u} \cdot \nabla \mathbf{u}\right) = -\nabla p + \frac{1}{\mathrm{Re}} \nabla^2 \mathbf{u} \tag{2.26}$$

Equation 2.26 shows that two different flow fields with unequal velocities and dimensions can still be *dynamically similar*, if their Reynolds numbers are equal. Then, the solution of one in dimensionless form will truly hold for the other.

Extending the scaling analysis further, the non-Darcy equations in coordinate-free form read as follows:

$$\frac{1}{\varepsilon}\left(\frac{\partial \mathbf{u}}{\partial t} + \frac{1}{\varepsilon}\mathbf{u} \cdot \nabla \mathbf{u}\right) = -\nabla p - \frac{1}{\mathrm{Re} \times Da}\mathbf{u} - \frac{f}{\sqrt{Da}}\mathbf{u}|\mathbf{u}| + \frac{1}{\varepsilon \mathrm{Re}} \nabla^2 \mathbf{u} \tag{2.27}$$

Here, Da, the Darcy number is defined as

$$Da = \frac{K}{L^2} \text{ while} f = \frac{1.8}{(180\varepsilon^5)^{0.5}}\varepsilon$$

Apart from Reynolds number, ε, Da, and f appear as additional dimensionless parameters in the formulation. For a given Reynolds number, the flow details will

then depend primarily on porosity, permeability, and the inertia coefficient; correspondingly, the flow distribution will depend on the dimensionless parameters of the formulation including ε, Da, and f.

2.4.2 Special Cases

The non-Darcy model is quite complex in its general form, but can be simplified in many circumstances. For steady flow, the dependence on time can be dropped, namely

$$\frac{\partial \mathbf{u}}{\partial t} = 0$$

When the flow is fully developed, the acceleration terms can be set to zero; hence

$$\left(\frac{\partial \mathbf{u}}{\partial t} + \frac{1}{\varepsilon}\mathbf{u} \cdot \nabla \mathbf{u}\right) = 0$$

Accordingly, one solves the following system of equations for the flow field:

$$0 = -\nabla p - \frac{1}{\mathrm{Re} \times Da}\mathbf{u} - \frac{f}{\sqrt{Da}}\mathbf{u}|\mathbf{u}| + \frac{1}{\varepsilon \mathrm{Re}}\nabla^2 \mathbf{u}$$

Additional simplifications may arise from the reduced dimensionality of the flow field. It is also clear that for small Reynolds numbers, the square-law dependence on velocity can be dropped; hence

$$\mathrm{Re} << 1, \quad -\nabla p - \frac{1}{\mathrm{Re} \times Da}\mathbf{u} + \frac{1}{\varepsilon \mathrm{Re}}\nabla^2 \mathbf{u} = 0$$

Equating the second and the third terms, the boundary-layer thickness δ near a solid wall can be estimated as

$$\frac{\delta}{L} \sim \sqrt{\frac{Da}{\varepsilon}}$$

Hence, in low permeability porous media $(Da << 1)$, the boundary-layer thickness is small and the corresponding wall shear stress term can be omitted in the calculation of the flow field outside the boundary layer. Thus, under the twin approximations of low Reynolds number and low permeability, we recover Darcy's law as the valid form of the momentum equation:

$$\mathrm{Re} << 1,\ Da << 1 : -\nabla p - \frac{1}{\mathrm{Re} \times Da}\mathbf{u} = 0$$

The above equation will be adequate for pressure drop calculations but will not resolve the wall boundary layers.

2.4.3 Compressible Flow

Compressible flow of a liquid in a Darcian framework is discussed in Sect. 2.1.3 in terms of a fluid property, namely compressibility. The present discussion generalizes this approach for a non-Darcy model.

Compressibility of the fluid in the porous region introduces fundamental changes in the mathematical equations relative to the incompressible formulation. Specifically, the mass balance equation is used to determine fluid density while the equation of state determines pressure. For a gas, changes in pressure take place simultaneously with temperature that must be introduced as a dependent variable. Thus, mass, momentum, and energy equations are coupled and are to be simultaneously solved. While working with compressible flow, it is common to introduce auxiliary-dependent variables such as enthalpy and entropy, depending on the application of interest. For example, when shocks are formed, large changes in entropy take place and it is advantageous to introduce entropy as a dependent variable.

The present discussion is restricted to gas flow in a fixed porosity porous region where compressibility arises from high gas speeds and hence, large changes in pressure. The fluid medium is taken to be an ideal gas so that the following equation of state, connecting pressure, density, and temperature, is applicable:

$$\frac{p}{\rho} = RT \tag{2.28}$$

In view of large changes in specific heat $C_p(T)$ of the gas, it is preferable to work with enthalpy h that relates to temperature as

$$C_p(T) = \left.\frac{\partial h}{\partial T}\right|_p$$

For high speed flow of compressible gas in a homogeneous region with no chemical reactions and shaft work, the governing equations are of mass, momentum, and energy (first law of thermodynamics), stated as follows [20]:

$$\begin{aligned}
&\frac{\partial \rho}{\partial t} + \nabla \cdot \rho \mathbf{u} = 0 \\
&\rho\left(\frac{\partial u}{\partial t} + \mathbf{u} \cdot \nabla \mathbf{u}\right) = -\nabla p + \nabla \cdot \left(\mu\left(\nabla \mathbf{u} + \nabla \mathbf{u}^T\right) - \frac{2}{3}\delta_{ij} \nabla \cdot \mathbf{u}\right) \\
&\rho\left(\frac{\partial e}{\partial t} + \mathbf{u} \cdot \nabla e\right) = \nabla \cdot \left(\frac{k}{C_p}\right) \nabla e \qquad \left(e = h + \frac{\mathbf{u}^2}{2}\right)
\end{aligned} \tag{2.29}$$

In this approach, the momentum equations solve for velocity, mass balance for density, energy equation for enthalpy and temperature while pressure is determined form the equation of state (2.28). Nevertheless, the system of equations is tightly coupled and must be jointly solved for the dependent variables. Since compressibility effects arise jointly with high speed flow of the gaseous medium, inertia effects in the momentum equation and advection terms in the energy equation become prominent. Equation 2.29 can then be simplified by dropping the viscous terms in the momentum equation and diffusion terms in the energy equations. These approximations considerably reduce the effort required to solve the governing equations.

Energy equation for a porous region is discussed in Sect. 2.5. The compressible flow equations as applied for a porous medium are subsequently revisited in Sect. 2.5.2.

2.4.4 Turbulent Flow

The overall effect of the solid grains of a porous matrix is to stabilize flow by increasing viscous forces uniformly throughout the physical domain. Conversely, when the pore size becomes large, the pore-scale Reynolds number can be substantial, leading to persistent unsteadiness in the local flow field. Boundary-layer thickness near an impermeable wall is small in a dense porous medium, scaling with $\sqrt{K}$ (K being the permeability). This change in boundary-layer thickness suggests a delay in the transition to turbulence [21]. To a first approximation, it can now be assumed that large-scale vortices of the size of the boundary-layer thickness do not appear in the porous medium. It is likely that the main sources of turbulence are then (i) vortex formation from the surface of the solid particles and (ii) shear layer instability in the pore space. The respective length scales of the turbulent fluctuations are then the particle diameter and the pore diameter [22, 23]. With the size of the REV much greater than either of these scales, the effect of fluctuations on flow distribution and pressure drop will have to be factored in through the time domain statistics.

While resolving every timescale present in the time-dependent fluctuations of velocity can be numerically difficult, a Reynolds-averaging approach can be attempted for turbulent flow. This step follows volume-averaging over REV that is intrinsic to the mathematical modeling of flow in porous media [24]. The

time-averaged flow field is now modified by Reynolds stresses that are temporal correlations of the velocity fluctuation vector. Combined with the Boussinesq approximation of turbulent viscosity, one obtains a modified form of the momentum equation wherein fluid viscosity is replaced by the sum of fluid viscosity and an eddy (or, turbulent) viscosity.

The time-averaged approach to modeling of turbulent flow ensures that the overall (time-averaged) pressure drop is correctly predicted for a given flow rate. In the process, instantaneous changes in velocity and pressure, particularly in the pores, are not fully resolved. The non-Darcy model accounts for the Darcian pressure drop arising from the interfacial friction between the fluid and solid phases, viscous friction within the fluid medium via the Brinkman correction, and flow separation effects including vortex shedding through the Forschheimer terms. Additional corrections for the turbulent fluctuations will necessarily represent those at the small scales within the pores of the porous medium. These effects, particularly vortex formation and turbulent fluctuations, are overlapping. As a result, modeling parameters of turbulent flow in porous media will be distinct from a homogeneous fluid and must be individually obtained from dedicated experiments of parameter estimation.

Following Eq. 2.27, the momentum equation governing turbulent flow in a porous medium can be written as

$$\frac{1}{\varepsilon}\left(\frac{\partial \mathbf{u}}{\partial t}+\frac{1}{\varepsilon}\mathbf{u}\cdot\nabla\mathbf{u}\right)=-\nabla p-\frac{1}{\mathrm{Re}\times Da}\mathbf{u}-\frac{f}{\sqrt{Da}}\mathbf{u}|\mathbf{u}| + \frac{1}{\varepsilon\mathrm{Re}}\nabla\cdot\left(1+\frac{\mu_T}{\mu}\right)\nabla\mathbf{u}$$

Here, velocities and pressure are both REV- and time-averaged. Symbol μ_T represents turbulent viscosity and is zero below a certain threshold Reynolds number. The continuity equation in terms of the time-averaged velocity will be applicable for mass conservation. Following the discussion on dispersion of Sect. 2.5, turbulent viscosity can be obtained as

$$\frac{\mu_T}{\mu}=C\mathrm{Re}_l, \mathrm{Re}_l>100 \text{ and } 0, \text{otherwise}$$

Here, Reynolds number is based on a pore-scale dimension and the average fluid speed. The constant of proportionality is expected to be of the order of unity. Here, turbulent fluctuations are taken to be present at the pore scale and create viscosity-like effects seen in jets and wakes. Correlations of turbulent viscosity similar to the one above can be seen in the context of round jets [25, 26]. Higher-order turbulence models (such as $k-\varepsilon$) in porous media have been discussed in the literature [27].

In heat and mass transfer, a non-participating solid phase merely creates a tortuous flow path. Combined with velocity fluctuations, the net influence on transport is to increase dispersion. See discussion accompanying Eq. 2.33 in Sect. 2.5.

Consider a thermally participating medium where the solid phase thermal conductivity is much greater that of the fluid phase. Thermal fluctuations are then uniformly damped within the porous medium (Eq. 2.33 of Sect. 2.5). The effect of turbulence on thermal transport will then be a function of the solid-to-fluid thermal conductivity ratio.

2.5 Energy Equation

Convective heat transfer in a porous region is the subject of discussion here. For a homogeneous fluid, the equation governing heat transfer is derived from the first law of thermodynamics [28]. The following assumptions greatly simplify the governing equation for temperature. These are:

i. Incompressible flow
ii. Constant fluid properties that are independent of temperature
iii. Negligible viscous dissipation
iv. No shaft work (or devices)
v. No heat generation
vi. No radiative fluxes

For a homogeneous fluid region, the governing equation is expressed as [29]

$$\rho C\left(\frac{\partial T}{\partial t}+\mathbf{u}\cdot\nabla T\right)=k\nabla^2 T$$

Here, ρ is fluid density, C is specific heat, and k is thermal conductivity. This form of the energy equation can be extended to a porous medium carrying fluid flow. The additional approximations needed to set up the energy equation in a homogeneous isotropic porous region are as follows.

1. The symbol $T(x,y,z,t)$ represents the REV-averaged temperature of the fluid and the solid phases jointly. Thus, the phases are at equal temperatures within the REV, for all time instants, an assumption referred as one of *thermal equilibrium*.
2. The time derivative refers to the change in sensible energy of the porous medium within the REV. Hence, the multiplying factor is $(\rho C)_m$ determined for the porous medium.
3. The advection term refers to energy transfer by the fluid phase. Hence, the multiplier is $(\rho C)_f$ as appropriate for the fluid phase.
4. On the right-hand side, thermal conductivity will be the effective medium conductivity (also called, *the stagnant medium* conductivity), denoted as k_m.
5. Heat conduction in a porous medium continues to be given Fourier's law

$$\mathbf{q} = -k_m \nabla T$$

Thus, the thermal energy equation in the porous medium can be expressed as

$$(\rho C)_m \frac{\partial T}{\partial t} + (\rho C)_f \mathbf{u} \cdot \nabla T = k_m \nabla^2 T \tag{2.30}$$

Expressions relating thermophysical properties of the solid and the fluid phases with those of the medium have been extensively discussed in the literature [9, 15, 30]. These depend on the individual properties, porosity, and the pore structure. The simplest correlations for specific heat and thermal conductivity of the porous region are given by the rule of mixtures:

$$(\rho C)_m = \varepsilon(\rho C)_f + (1-\varepsilon)(\rho C)_s$$
$$k_m = \varepsilon k_f + (1-\varepsilon)k_s$$

Here, f and s refer to the fluid and the solid phases while m is the porous medium. Effective (equivalent) thermal conductivity of the porous medium is related to the direction of the temperature gradient, and the expression above is to be seen as an upper limit when the solid and the fluid phases are in series. A parallel arrangement of the phases yields the lower limit as

$$\frac{k_m}{k_f} = \frac{k_s/k_f}{(1-\varepsilon) + \varepsilon k_s/k_f}$$

The effective thermal conductivity of a sufficiently dilute suspension $(\varepsilon \to 1)$ with spherical particles is given by the analytically derived Maxwell model:

$$\frac{k_m}{k_f} = \frac{(3-2\varepsilon)k_s/k_f + 2\varepsilon}{3 - \varepsilon + \varepsilon k_s/k_f}$$

An equivalent expression with the solid phase treated as a collection of cylinders (wires) is given by the Rayleigh model:

$$\frac{k_m}{k_f} = \frac{1 + k_s/k_f - (1-\varepsilon)(1-k_s/k_f)}{1 + k_s/k_f + (1-\varepsilon)(1-k_s/k_f)}$$

Other models for non-periodic geometries and non-spherical particles are presented in the literature, but the effective medium conductivity is a source of uncertainty in transport modeling in porous media. In general, these can be derived mainly from experiments. In a gas–metal system (as in Chap. 6), the medium properties are closely aligned with the metallic phase with $(1-\varepsilon)$, namely (1—porosity) as a multiplier. For temperature-dependent thermal conductivity, the right side of Eq. 2.30 is written as $\nabla \cdot (k_m(T)\nabla T)$.

For anisotropic and inhomogeneous porous media, thermal conductivity is a second-order tensor (like permeability in Sect. 2.1.2), and the energy equation is written as

$$(\rho C)_m \frac{\partial T}{\partial t} + (\rho C)_f \mathbf{u} \cdot \nabla T = \nabla \cdot [k_m] \nabla T \tag{2.31}$$

Fluid velocity in these expressions continues to be the Darcian velocity evaluated for the REV as a whole. At the scale of the REV, the real flow path tends to be tortuous, thus increasing the possibility of intermixing of the hot and the cold fluid streams and greater spreading. This effect will show up as an augmentation of thermal conductivity and is referred as *dispersion* (Fig. 2.3). Since velocity has three components, dispersion can occur in three dimensions. Equation 2.31 is now written to include a dispersion tensor, also called dispersion coefficient D_m as

$$(\rho C)_m \frac{\partial T}{\partial t} + (\rho C)_f \mathbf{u} \cdot \nabla T = \nabla \cdot [k_m + D_m] \nabla T \tag{2.32}$$

Here, dispersion augments molecular conduction and so the elements of the dispersion tensor are positive. Experiments in homogeneous isotropic porous media show that dispersion tensor reduces to a scalar quantity and is related to fluid speed as [31, 32]:

$$d_m = (\rho C)_m l |\mathbf{u}| \text{ where}$$
$$l = \text{constant} \cdot d_p (Pe_d < 1); l = CPe_d^n \cdot d_p (Pe_d > 1), 0 < n < 1$$

Symbol l is called *dispersion length,* and d_p is the particle diameter. Peclet number is defined in this context as

$$Pe_d = \frac{|\mathbf{u}| d_p}{\alpha_f}$$

Here, α_f is the fluid thermal diffusivity.

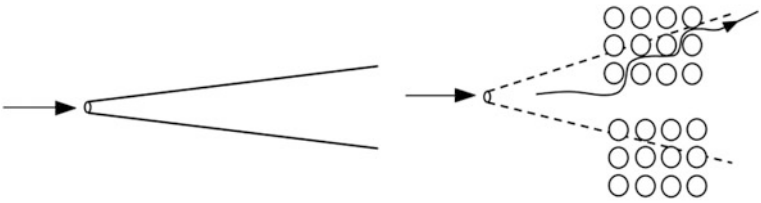

Fig. 2.3 Schematic drawing of tortuosity and dispersion in a porous medium; (left) spread of thermal energy from a line source in a homogeneous fluid phase; (right) higher spread in a porous medium arising from tortuosity of the flow path

Let U be the velocity scale, L the length scale, and the property ratios defined as

$$\tilde{\beta} = \frac{(\rho C)_f}{(\rho C)_m} \quad \lambda = \frac{k_f}{k_s}$$

The dimensionless form of the thermal energy equation with constant dispersion is written as

$$\frac{\partial T}{\partial t} + \tilde{\beta}\mathbf{u} \cdot \nabla T = \nabla \cdot \left(\frac{1}{Pe} \nabla T\right) \tag{2.33}$$

Peclet number appropriate for the scale of the entire porous medium is now defined as

$$Pe = \frac{UL}{\alpha_{mol} + \alpha_m}$$

The molecular thermal diffusivity in the definition of Pe is

$$\alpha_{mol} = \frac{k_m}{(\rho C)_m}$$

while the dispersion part is

$$\alpha_m = \frac{d_m}{(\rho C)_m} = l|\mathbf{u}| \sim lU$$

In the presence of turbulent fluctuations in the pores of the physical region, the dispersion length is further augmented by an amount, constant $\times$ pore diameter (Sect. 2.4.4), where the constant value is to be determined from reference experiments. Being dimensionless, the constant will scale with the fluid Prandtl number. It is understandable that velocity and temperature fluctuations will correlate for small Prandtl numbers as in liquid metals. For $Pr \geq 1$, this dependence can be expected to be small [25]. For small fluid-to-solid thermal conductivity ratio λ, thermal fluctuations will be damped by the solid phase.

The thermal energy equation requires specification of additional parameters over and above the flow field itself. Being a second-order partial differential equation in space, boundary conditions must also be specified. As in the modeling of pressure and velocity, these are classified as Dirichlet (temperature specified), Neumann (heat flux specified), and Robin (linear combination of temperature and heat flux specified). For unsteady heat transfer problems, an initial condition is required for the temperature calculation within the porous medium.

2.5.1 Thermal Non-equilibrium Model

The assumption of equal phase temperatures is equivalent to requiring the fluid and the solid media attain local thermal equilibrium quickly, in relation to the overall timescale of the transport process. This assumption is violated in several contexts and more so during rapid transients, namely when the timescale of the superimposed process is itself small.

An explicit treatment of individual phase temperatures is more general and will contain the approximation of thermal equilibrium as a special case. In view of this generality, the thermal non-equilibrium model is presented below. It is assumed that the porous medium has a solid phase coexisting with a single continuous fluid phase, leading to the two-equation model for temperature. These equations solve for the fluid and solid phase temperatures.

The respective equations will resemble the energy equations at the pure fluid and the pure solid limits with a point of difference. For the fluid medium, the solid particles at a distinct temperature will serve as an energy *sink* (or *source*, depending on the sign of the local temperature difference). One can imagine a hot fluid entering a cold porous region; a substantial part of the fluid energy will be spent in warming up the solid phase. This process requires a temperature difference and, clearly, a non-equilibrium model. The fluid–solid energy exchange term is thus central to the two-equation formalism.

The fluid phase energy equation for temperature T^f is written as:

$$\varepsilon(\rho C)_f\left(\frac{\partial T^f}{\partial t}+\frac{\mathbf{u}}{\varepsilon}\cdot\nabla T^f\right)=k_f\nabla^2T^f+Q_{f\leftarrow s} \tag{2.34}$$

Similarly, the energy equation for the solid phase is written in terms of temperature T^s as

$$(1-\varepsilon)(\rho C)_s\left(\frac{\partial T^s}{\partial t}\right)=k_s\nabla^2T^s+Q_{f\rightarrow s} \tag{2.35}$$

Comparing Eqs. 2.34 and 2.35, the following points of difference may be noted:

(a) The heat capacity term for the fluid is multiplied by porosity which is the volume fraction of the fluid phase. The corresponding term in the solid phase equation is multiplied by (1-porosity), the volume faction of the solid phase. This is understandable because the two equations are jointly applicable for a unit volume of the porous medium.
(b) The fluid temperature equation is written exclusively in terms of its thermophysical properties. The solid phase equation employs its own conductivity, density, and specific heat. It is assumed here that, within the REV, the two phases are adequately connected with independent paths for heat transfer.

(c) Since energy exchange at the phase boundary is continuous at all time instants, the source terms $Q_{f\to s}$ and $Q_{f\leftarrow s}$ are equal in magnitude but opposite in sign.

Equations 2.34 and 2.35 can be used in modeling only after the source terms are prescribed. Assuming a convective heat transfer environment, the source term, evaluated per unit volume of the REV, can be written as

$$Q_{f\to s} = hA_{IF}(T^f - T^s) \tag{2.36}$$

Similarly

$$Q_{f\leftarrow s} = hA_{IF}(T^s - T^f)$$

The heat transfer coefficient between the two phases is denoted as h and A_{IF}, the *specific area*, is the interfacial area per unit volume of the porous medium (units of m^{-1}). The specific area will depend on the pattern of arrangement of the solid phase within the fluid. Heat transfer coefficient can be determined from Nusselt number correlations such as

$$Nu = \frac{hL}{k_f} = APe^m$$

The diffusion term in Eq. 2.34 can be rewritten to include dispersion as

$$\nabla \cdot (k_f + d_f)\nabla T = \nabla \cdot (k_{eff})\nabla T$$

Using uniform velocity and length scales U and L for the two temperature equations, a timescale of L/U, and $Pe = UL/\alpha_f$, the dimensionless form of the thermal non-equilibrium model is summarized as follows:

$$\text{FLUID:}\quad \varepsilon\left(\frac{\partial T^f}{\partial t} + \frac{\mathbf{u}}{\varepsilon}\cdot\nabla T^f\right) = \frac{1}{Pe}\nabla\cdot\left(\frac{k_{eff}}{k_f}\right)\nabla T^f - \frac{NuA_{IF}}{Pe}(T^f - T^s) \tag{2.37}$$

$$\text{SOLID:}\ (1-\varepsilon)\left(\frac{\partial T^s}{\partial t}\right) = \frac{\beta/\lambda}{Pe}\nabla^2 T^s + \frac{NuA_{IF}\beta}{Pe}(T^f - T^s) \quad \text{where } \beta = \frac{(\rho C)_f}{(\rho C)_s} \tag{2.38}$$

Symbol λ is the fluid-to-solid thermal conductivity ratio. An application of the two-equation model is presented in Chap. 6 for oscillatory flow in metallic mesh regenerators.

The two-equation model of heat transfer will reduce the thermal equilibrium model when the energy exchange term of Eq. 2.36 is zero. This limit is reached

when the heat transfer coefficient is large, indicating $T^f - T^s \to 0$, i.e., an equality of phase temperatures. Alternatively, the solid phase conductivity can approach zero, thus decoupling the solid and fluid phase temperatures. In this respect, the thermal equilibrium model also holds for a thermally non-participating solid phase whose role is entirely to create a tortuous flow path for the fluid medium.

Effective thermal conductivity in Eq. 2.37 will have to be augmented for additional dispersion in turbulent flow. Temperature fluctuations will be damped by a highly conducting solid phase, and this correction will not be required. In a solid phase of low conductivity, a single-equation model of heat transfer will be adequate. Here, the correction for turbulent fluctuations will be as per the discussion accompanying Eq. 2.33 (Sect. 2.5).

2.5.2 Compressible Flow

Following the discussion of Sect. 2.4.3, we examine the mass, momentum, and energy equations of high speed gas flow in a porous medium whose pore geometry as well as the solid particles is rigid. Mechanical work and viscous dissipation terms are neglected in the fluid phase energy equation with the expectation that the fluid–solid energy exchange terms would be dominant. Total energy, the sum of enthalpy and kinetic energy is approximated as enthalpy since velocities expected within a porous medium will not be excessive. Enthalpy is written as the product of (ρC) and T, for each of the two phases. A non-Darcy, two-equation thermal non-equilibrium model is proposed here, and the following system of equations can be derived:

$$\begin{aligned}
&\text{Mass} : \varepsilon\frac{\partial \rho}{\partial t} + \nabla\cdot(\rho\mathbf{u}) = 0\\
&\text{Momentum} : \frac{\rho}{\varepsilon}\left(\frac{\partial \mathbf{u}}{\partial t} + \frac{1}{\varepsilon}\mathbf{u}\cdot\nabla\mathbf{u}\right) = -\nabla p - \frac{\mu}{K}\mathbf{u} - \frac{\rho F}{\sqrt{K}}\mathbf{u}|\mathbf{u}| + \frac{\mu}{\varepsilon}\nabla^2\mathbf{u}\\
&\text{Fluid} : \varepsilon\left(\frac{\partial(\rho C)_f T^f}{\partial t} + \nabla\cdot(\rho C)_f\frac{\mathbf{u}}{\varepsilon}T^f\right) = \nabla\cdot\left(\frac{k_{eff\,f}}{C_f}\nabla(C_f T^f)\right) + Q_{f\leftarrow s}\\
&\text{Solid} : (1-\varepsilon)\left(\frac{\partial(\rho C)_s T^s}{\partial t}\right) = \nabla\cdot\left(\frac{k_s}{C_s}\nabla(C_s T^s)\right) + Q_{f\to s}
\end{aligned} \tag{2.39}$$

The fluid–solid energy exchange term is given by Eq. 2.36. The left side of the fluid phase energy equation can be simplified using the mass balance equation as

$$\varepsilon\left(\frac{\partial(\rho C)_f T^f}{\partial t} + \nabla\cdot(\rho C)_f\frac{\mathbf{u}}{\varepsilon}T^f\right) = \varepsilon\rho_f\left(\frac{\partial(C_f T^f)}{\partial t} + \frac{\mathbf{u}}{\varepsilon}\cdot\nabla(C_f T^f)\right)$$

The form on the right side is convenient for discretization in numerical simulations. The product of specific heat and temperature can be treated as a single dependent variable. The temperature formulation is, however, to be preferred since the energy exchange term is presented in the form the phase temperature difference. Specific heat as a function of temperature for the participating phases is independently supplied as constitutive equations in the model. Thus, in the system given by Eq. 2.39, the mass balance equation determines density, momentum equation solves for the Darcian velocity, the energy equations yield the fluid and solid phase temperatures, and the ideal gas equation of state will determine the fluid phase pressure. For a discussion on compressible flow through a deformable porous medium and formation of shock waves, see [33, 34].

2.6 Unsaturated Porous Medium

In the discussion of Sects. 2.1–2.5, the pore space was taken to be filled with a single fluid, thus making the porous medium saturated. Consider flow of water in a porous medium with air pockets around. An example is groundwater flow, where water may not fill the available pore space. Such a medium is said to be *unsaturated*. Applications involving unsaturated flow are quite a few. A variable that characterizes the volume fraction of the liquid in the pore space available within the porous medium is *saturation* and is denoted as S. In the context of groundwater, the symbol adopted is S_w to indicate water saturation. The volume fraction of air in such an instance is $1 - S_w$.

An important consequence of the porous medium being unsaturated is the appearance of interfacial forces. Figure 2.4 shows a porous medium partially saturated with water. Assuming that the solid phase is wetted by water, a meniscus will form within the pore space, as shown schematically in Fig. 2.4. A simple balance of forces at the interface shows that, under equilibrium conditions, pressure in the liquid phase will be smaller than that in the gaseous phase, namely $p_w < p_a$..

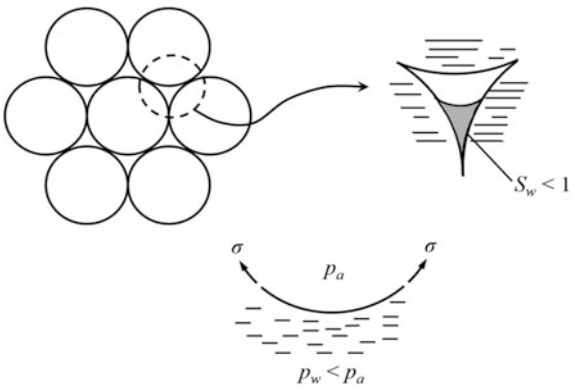

Fig. 2.4 Formation of interfaces and the importance of surface tension in an unsaturated porous medium containing air and water. As shown, water wets the solid surface and is called the *wetting* phase

The difference is balanced by the appropriate component of surface tension integrated over the wetting perimeter. The difference will scale with the interface curvature, increasing as the pore size diminishes and decreasing with higher water content in the pores.

Suppose the quantity of interest is flow of water, for example, the speed with which it saturates the porous medium. To a first approximation, we may assume here that the gaseous phase, a mixture of air and moisture, will be practically at the atmospheric pressure. To mobilize water, an extra pressure will have to be provided at one end of the porous region. Flow is setup when the excess pressure overcomes the force of surface tension at the water–air–grain three-phase boundary.

An exact analysis of interfacial forces in a porous medium is formidable, and more so because it depends on the geometry of the pore space. Instead, analysis can proceed on the scale of the REV, and one can write the revised form of Darcy's law, applicable for a phase ϕ of an unsaturated porous medium as follows [35, 36]:

$$\mathbf{u}^{\phi} = -k_r(S_{\phi})\frac{K}{\mu}\nabla p^{\phi} \tag{2.40}$$

Comparing with Eq. 2.1, it is clear that the difference in formulation arises from the function k_r, called the *relative permeability*. It is a dimensionless quantity. Since the formation of interfaces increases flow resistance, it can be surmised that the relative permeability function will be smaller than unity. When water is withdrawn from the pores, the interface curvature steepens, increasing the flow resistance further. Thus, relative permeability is a function of the phase saturation, a functionality shown in Eq. 2.40.

In a porous medium with two fluids 1 and 2 jointly present, Eq. 2.40 is written as follows:

$$\begin{aligned}\mathbf{u_1} &= -k_{r1}(S_1)\frac{K}{\mu_1}\nabla p_1\\ \mathbf{u}_2 &= -k_{r2}(S_2)\frac{K}{\mu_2}\nabla p_2\end{aligned} \tag{2.41}$$

Here, $S_1 + S_2 = 1$. For air–water flow, air may be taken to be at the atmospheric pressure, namely $p_2 \approx p_{atm}$ leading to zero velocity in the gaseous phase. Equation 2.41 then reduces to a single momentum equation for the migration of water:

$$\mathbf{u}_w = -k_r(S_w)\frac{K}{\mu_w}\nabla p_w$$

Equations 2.40 and 2.41 are momentum equations for unsaturated flow in porous media. The restrictions applicable for Darcy's law continue to hold, namely the pore-scale Reynolds number is less than unity. This approximation is quite acceptable in many instances since fluid speeds are smaller under unsaturated conditions.

The phase pressures are, in turn, determined with reference to the mass balance equation for an unsaturated medium. The discussion is initially for air–water flow where air is the stagnant phase. Water saturation is denoted as S_w, ρ is water density, and $\mathbf{u}$ is the Darcian velocity of water averaged over the REV. Start with the general form of the mass balance equation for the liquid contained in the pores of the physical region. Hence

$$\frac{\partial}{\partial t}(\varepsilon \rho S_w) + \nabla \cdot \rho \mathbf{u} = 0$$

The product of porosity and water saturation arises from the fact that saturation is defined with respect to the pore volume. Treating water as incompressible (ρ = constant) and porosity as constant, the mass balance equation simplifies to

$$\varepsilon \frac{\partial S_w}{\partial t} + \nabla \cdot \mathbf{u} = 0 \tag{2.42}$$

Using Eq. 2.41 for velocity, the pressure equation can be derived as

$$\varepsilon \frac{\partial S_w}{\partial t} = \frac{\partial}{\partial x}\left(\frac{k_r(S_w)K}{\mu_w}\frac{\partial p_w}{\partial x}\right) \tag{2.43}$$

Permeability K and water viscosity μ_w are independently prescribed quantities. Relative permeability is a function of water saturation and is a characteristic property of the porous medium. It is to be specified from experimental characterization of the medium under study. Since water migration in unsaturated soils is a slow process, quasi-static conditions may be assumed to hold. The pressure difference across the interface between the non-wetting and the wetting phases, called the *capillary pressure* (p_c), will be function of the interface shape and liquid volume. To a first approximation, this dependence can be linked with the local saturation [37]. Thus, for air–water flow (Fig. 2.4), capillary pressure, a positive quantity, is given as

$$p_c = p_a - p_w = g(S_w)$$

Typical variations of relative permeability with saturation and saturation with capillary pressure are shown in Fig. 2.5.

Equation 2.43 can be written entirely in the form of a second-order nonlinear PDE for water pressure as follows:

$$-\varepsilon \frac{dS_w}{dp_c}\frac{\partial p_w}{\partial t} = \frac{\partial}{\partial x}\left(\frac{k_r(S_w)K}{\mu_w}\frac{\partial p_w}{\partial x}\right) \tag{2.44}$$

Equation 2.44 will determine phase pressure in water, and fluid velocity can be determined from Darcy's law (Eq. 2.41). The derivative of water saturation with

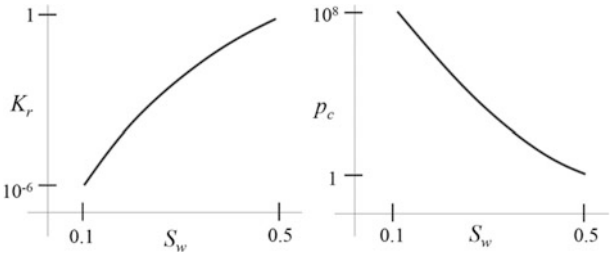

Fig. 2.5 Variation of relative permeability with water saturation and saturation with capillary pressure (arbitrary units) in clay-type porous media

capillary pressure is negative (see Fig. 2.5). With this comment, Eq. 2.44 is in the form of a nonlinear diffusion equation [38].

Under non-isothermal conditions, it is possible to identify distinct temperatures for the fluid phases and one for the solid phase. In a thermal equilibrium model, the three are assigned a single volume-averaged temperature and Eq. 2.32 carries over. Effective medium properties of thermal capacity and thermal conductivity are now functions of the local saturation.

Extensions of the formulation for unsaturated flow with two or more fluids are discussed in the following sections.

2.6.1 Oil–Water Flow

As an immediate extension of unsaturated flow of water in a partially wet porous region, immiscible flow of oil and water in a porous medium is now considered. The context is an application of enhanced oil recovery from oil-rich reservoirs. Pressurized water serves to mobilize oil trapped in the pores of the host rock. Heating the injected water also serves to lower oil viscosity and decrease flow resistance. The physical picture outlined in the previous section carries over. Oil and water form an interface, and surface tension creates a jump in pressure across this boundary. Thus, the two fluid phases move under the influence of the respective phase pressures. Unlike air that was taken to be at the atmospheric pressure, water and oil are in motion, leading to a spatiotemporal variation in the fluid pressures. The overall approach of using relative permeability to augment flow resistance and deriving capillary pressure from saturation continues to be applicable. As expected, these equations are nonlinear, and specialized numerical methods are needed for their solution. The subject of oil–water flow has been extensively studied over the years, and several references can be seen in the list at the end of the chapter [39–42].

Mass balance: The mass balance equation is written for oil and water as follows:

$$\text{Oil} : \frac{\partial}{\partial t}(\varepsilon \rho_o S_o) + \nabla \cdot (\rho_o \mathbf{u}_o) = 0 \tag{2.45a}$$

$$\text{Water} : \frac{\partial}{\partial t}(\varepsilon \rho_w S_w) + \nabla \cdot (\rho_w \mathbf{u}_w) = 0 \tag{2.45b}$$

Specifying that that the pores contain water and oil and no other fluid, we get

$$S_o + S_w = 1 \tag{2.46}$$

Momentum equation: Assuming the fluid velocities to be reasonably small, the momentum equation is a form of the generalized Darcy's law that includes a correction by the relative permeability. For oil and water, these are expressed as follows:

$$\text{Oil} : \mathbf{u}_o = -\frac{k_{ro}(S_o)K}{\mu_o} \nabla p_o \tag{2.47a}$$

$$\text{Water} : \mathbf{u}_w = -\frac{k_{rw}(S_w)K}{\mu_w} \nabla p_w \tag{2.47b}$$

The momentum equations can be combined with the mass balance equations to arrive at a single nonlinear second-order partial differential equation in pressure for each of the two phases. Here, the temperature field (REV-averaged) is taken to be evolving in space and time so that the fluid properties—density and viscosity—are non-constant. Fluid compressibility with respect to pressure and temperature is defined as:

$$\xi = \left.\frac{\partial \rho}{\partial p}\right|_T ; \qquad \zeta = \left.\frac{\partial \rho}{\partial T}\right|_p$$

The phase pressure equations can now be derived as:

$$\begin{aligned} &\text{Oil} : -S_o \zeta_o \frac{\partial T}{\partial t} + S_o \xi_o \frac{\partial p_o}{\partial t} - \frac{dS_w}{dp_c}\left[\frac{\partial p_o}{\partial t} - \frac{\partial p_w}{\partial t}\right] \\ &= \frac{1}{\rho_o} \nabla \cdot \left[\frac{K k_{ro} \rho_o}{\varepsilon \mu_o}\right] \nabla p_o \end{aligned} \tag{2.48a}$$

$$\begin{aligned} &\text{Water} : -S_w \zeta_w \frac{\partial T}{\partial t} + S_w \xi_w \frac{\partial p_w}{\partial t} - \frac{dS_w}{dp_c}\left[\frac{\partial p_o}{\partial t} - \frac{\partial p_w}{\partial t}\right] \\ &= \frac{1}{\rho_w} \nabla \cdot \left[\frac{K k_{rw} \rho_w}{\varepsilon \mu_w}\right] \nabla p_w \end{aligned} \tag{2.48b}$$

Here, water is the wetting phase with oil, the non-wetting phase. Consequently, the capillary pressure, a positive quantity, is expressed as $p_c = p_o - p_w$ and $S_o + S_w = 1$. In an isothermal reservoir, derivatives of temperature can be set equal to zero.

Thermal energy equation: If the injected water is at a temperature higher than the oil-rich formation, a thermal front will move through the porous region. The front position can be determined by solving the appropriate form of the thermal energy equation. For the present discussion, an REV-averaged, thermal equilibrium model is proposed, wherein the fluid phases as well as the porous matrix are locally at the same temperature. This assumption is realistic because the fluid speeds in the reservoir are expected to be small, yielding time constants much larger than the fluid–solid equilibration time. Following Eq. 2.32, the thermal energy equation is written in Cartesian coordinates as:

$$\frac{\partial T}{\partial t} + U\frac{\partial T}{\partial x} + V\frac{\partial T}{\partial y} = \frac{K_h}{\sigma_T}\nabla^2 T \tag{2.49}$$

Here, the coefficients include the effective medium properties corrected for fluid saturation. These are respectively given as follows:

$$\begin{aligned} U &= \frac{u_o\rho_o C_o + u_o\rho_o C_o}{\sigma_T} \\ V &= \frac{v_o\rho_o C_o + v_o\rho_o C_o}{\sigma_T} \\ \sigma_T &= \varepsilon(S_o\rho_o C_o + S_w\rho_w C_w) + (1-\varepsilon)(\rho C)_R \end{aligned} \tag{2.50}$$

Symbol K_h represents the effective thermal conductivity of the porous medium filled with multiple fluids. As written in Eq. 2.49, dispersion is not considered since fluid speeds are small. If the variation in conductivity with saturation is included, thermal conductivity will no longer be spatially constant (see discussion in Sect. 2.5). The momentum equation is affected by temperature distribution, first through the explicit temperature terms, but this is usually a smaller influence. The real dependence emerges from large reduction in oil viscosity with increasing temperature.

The mass, momentum, and energy equations are to be supplemented with thermophysical properties of oil and water as well as the oil-bearing rock (marked *R*). In addition, the following constitutive relations specific to the site being analyzed are required:

$$\begin{aligned} k_{rw} &= k_{rw}(S_w) \\ k_{ro} &= k_{ro}(S_w) \\ p_c &= p_o - p_w = p_c(S_w) \\ \frac{\rho_i}{\rho_{ref}} &= 1 + \xi_i(p_i - p_{ref}) - \zeta_i(T_i - T_{ref}), i = \text{oil,water} \end{aligned} \tag{2.51}$$

Apart from the variability of porosity and permeability in a field-scale oil-bearing reservoir, parametric functions such as relative permeability and capillary pressure can also vary substantially and over several orders of magnitude (Fig. 2.5). Estimation of these functions in randomly inhomogeneous media is a formidable task and has been addressed in the literature [43–45].

The formulation given above is applicable for immiscible fluids. If fluids mix, the governing equations become more complicated owing to mass fluxes of one fluid into another [46]. The mass balance equation is itself modified by factors such as hydrodynamic dispersion, requiring significant reformulation of the equations of mass, momentum, and energy.

Initial and boundary conditions: The system of equations given above is coupled and can only be numerically solved. Simulation studies with such systems have been discussed in the literature by various authors [47–51]. Specific solutions can be obtained in selected geometries with known boundary conditions. Two configurations, one and two dimensional, respectively, are sketched in Fig. 2.6. In the one-dimensional simulation, oil and water pressures are specified on each side of the physical domain, temperature is prescribed on the left side, and a suitable *outflow* condition is applied on the right. Initial conditions for the phase pressures and temperature over the entire domain are also required. In two-dimensional simulation, the figure sketched is a quarter of a repeating geometry of injection and production wells. The former carries pressurized and heated water, while oil and water are recovered at the other end. Thus, pressures and temperature are prescribed at the injection well, shown in Fig. 2.6 as a quarter of a circle. Pressures and a suitable temperature outflow condition are prescribed at the production well. On other boundaries, the symmetry condition in the form of a zero normal derivative boundary condition is prescribed.

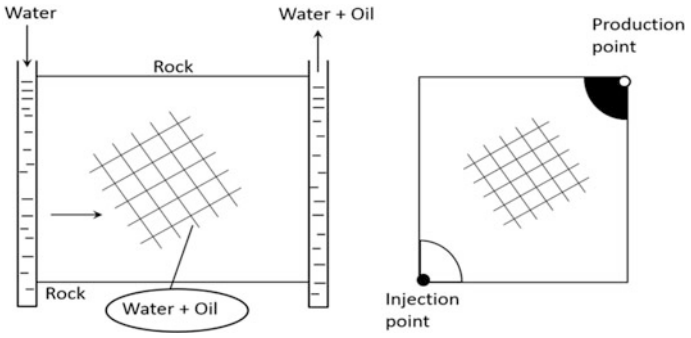

Fig. 2.6 One (left)- and two (right)-dimensional geometries chosen for simulation of enhanced oil recovery. In a two-dimensional geometry, water is injected at the injection well shown as a quarter-circle. Oil and water are recovered at the production well

2.6.2 Multiphase Multicomponent Flow

Generalizing oil–water flow in a porous medium, it is possible to imagine a scenario where gas, liquid, and solid fill the pore space while each phase has multiple chemical entities present. This is an example of multiphase, multicomponent flow and transport in a porous medium. As a specific example, a non-isothermal, multiphase, multispecies model is presented here for the simulation of CH_4 gas production via depressurization of a gas hydrate reservoir and simultaneous CO_2 injection [52–57]. The subject is discussed in detail in Chap. 7.

The porous medium in the present discussion is soil beneath water bodies such as lakes and oceans. In the pore space, all three phases—solid, liquid, and gas—are present. Each phase contains multiple species such as water and methane. The species balance equation, for example, of methane, is to be summed up over all the phases. The phase equilibrium relation brings in thermodynamic aspects in transport modeling. An example is the amount of methane present in the gas hydrate (solid) phase at a given pressure and temperature. Departure from equilibrium will result in reaction kinetics that will proceed at a speed in proportion to the distance from the equilibrium curve. The reaction chemistry is accompanied by stoichiometry, as discussed in Chap. 7 in the context of gas hydrates. In principle, each phase has its own pressure, temperature, and velocity. In the following discussion, the gas phase is treated to be ideal, local temperature to be equal among the phases including the solid matrix (thermal equilibrium) and solid phase velocity (soil as well as the hydrate deposits in the pores) to be zero.

The governing equations are written for simplicity in a one-dimensional Cartesian geometry bounded by the depressurization well at one end where methane is recovered and the injection well at the other where pressurized CO_2 can be introduced. The present model accounts for transport phenomena in the five components, namely aqueous, gas, CH_4-hydrate, CO_2-hydrate, and the geologic media, spread over three phases. While the first two components are mobile, the other three are treated as immobile. Such a distinction helps in accounting for the thermophysical properties of CH_4- and CO_2-hydrates. At a time instant and a given location, all five components present in the system are assumed to be in thermal equilibrium with each other. Temperature itself varies considerably over the spatial extent of the reservoir and is obtained as a part of the overall solution. The gas phase comprises a mixture of CH_4 and CO_2, while the liquid phase is aqueous and contains only H_2O. The solubility of CH_4 and CO_2 gases in the aqueous phase and the presence of H_2O in the gas phase can be shown to have small impact on gas recovery and is neglected.

Let subscripts 'g', 'mh', and 'ch' indicate gas, methane hydrate, and CO_2 hydrate, respectively. Superscripts 'm', 'c', and 'w' indicate methane, CO_2, and water, respectively. Let ω refer to mass fraction; thus ω_g^m stands for the mass fraction of methane in the gas phase. Similarly, the symbol ω_c^m is the mass fraction of CO_2 in the gas phase. Since these are the only two components of the gas phase, $\omega_g^m + \omega_c^m = 1$. Noting that methane is present in the gas phase as well as in methane

hydrate (a solid phase), a mass balance equation of methane cutting across phases will read as follows:

$$\text{Methane}\quad \varepsilon\frac{\partial}{\partial t}\left(\rho_g s_g \omega_g^m + \rho_{mh} s_{mh} \omega_{mh}^m\right) = -\frac{\partial}{\partial x}\left(\rho_g \omega_g^m v_g + J_g^m\right) + \dot{m}_g^m + \dot{m}_{mh}^m \tag{2.52}$$

The left side is a mass storage term of methane in the REV. The first term on the right includes the diffusive mass flux given by symbol J (Eq. 2.54 below) and the advective mass flux that depends on the gas speed. Both terms serve to transport methane through the porous region. The velocity field is assumed to be Darcian, and the momentum equation of each fluid phase (gas and liquid) is expressed in one-dimensional form as:

$$v_\gamma = -\frac{K_{abs} k_{r\gamma}}{\mu_\gamma}\frac{\partial P_\gamma}{\partial x}, \gamma = g, l \tag{2.53}$$

The diffusive mass fluxes of methane and CO_2 appearing in the gas phase mass transport equations are given by the Fick's law, namely:

$$J_g^i = -\phi \rho_g s_g D_g^i \frac{M^i}{M_g}\nabla(\chi_g^i), \quad i = m, c \tag{2.54}$$

The source terms in the mass conservation equation of methane include possible chemical reactions in the gas phase that produce methane $\left(\dot{m}_g^m\right)$ and formation/dissociation reactions that generate/consume methane from the hydrates in the solid phase $\left(\dot{m}_{mh}^m\right)$.

Extending this approach to CO_2, the mass conservation equation is written as

$$\phi\frac{\partial}{\partial t}\left(\rho_g s_g \omega_g^c + \rho_{ch} s_{ch} \omega_{ch}^c\right) = -\frac{\partial}{\partial x}\left(\rho_g \omega_g^c v_g + J_g^c\right) + \dot{m}_g^c + \dot{m}_{ch}^c \tag{2.55}$$

The mass conservation equation of water that constitutes the liquid phase is similarly written as:

$$\phi\frac{\partial}{\partial t}\left(\rho_l s_l \omega_l^w + \rho_{mh} s_{mh} \omega_{mh}^w + \rho_{ch} s_{ch} \omega_{ch}^w\right) = -\frac{\partial}{\partial x}\left(\rho_l \omega_l^w v_l\right) + \dot{m}_l^w + \dot{m}_{mh}^w + \dot{m}_{ch}^w \tag{2.56}$$

The symbols carry their usual meaning. From left to right, the right side of Eqs. 2.55 and 2.56 carries the advection velocity, diffusive mass flux, and mass source terms arising from chemical reactions.

Using a volume-averaged temperature over the REC covering the three phases, the thermal energy equation is written as:

$$\frac{\partial}{\partial t}\left[\sum_{\gamma=l,g,mh,ch}\left(\phi\rho_\gamma s_\gamma U_\gamma\right)+(1-\phi)\rho_s U_s\right]+\sum_{\gamma=l,g}\left[\sum_{i=m,c,w}\frac{\partial}{\partial x}\left(v_\gamma\rho_\gamma s_\gamma\omega_\gamma^i H_\gamma^i\right)\right]$$
$$+\sum_{i=m,c}\frac{\partial}{\partial x}\left(J_g^i H_g^i\right)=\frac{\partial}{\partial x}\left(K_{eq}\frac{\partial T}{\partial x}\right)+\sum_{\gamma=l,g,mh,ch}\left[\sum_{i=m,c,w}\frac{\partial}{\partial x}\left(\dot{m}_\gamma^i H_\gamma^i\right)\right]+\dot{E} \tag{2.57}$$

The index γ sums up contributions from the three phases; the index 'i' performs summation over the applicable species. Symbol $\dot{E}$ refers to heat released/absorbed during exothermic and endothermic reactions in the porous region. Symbol U is velocity with the solid phase velocity U_s being, usually, zero. Symbol H is used to indicate phase enthalpy of the appropriate species.

The closure of the set of governing equations requires applicable constitutive relations and reaction kinetics. Specific forms of the constitutive relations, kinetic data, and heat release function are given in Chap. 7.

2.7 Mass Transfer

Saltwater mixing with freshwater in soil and leaching of chemicals from buried containers are examples of mass transfer in porous media. The transport phenomenon referred here is of a solute, for example, salt in a solvent such as water from regions of high concentration toward the low. It is possible to envision this transfer as analogous to thermal energy, temperature being equivalent to solutal concentration [2, 5, 7–9, 58–60]. In this discussion, concentration (C; also called, *mass* concentration) is expressed in units of mass of the solute per unit volume of the solution (e.g., mg/l). The solution in the present discussion is *clear*, namely free of particulates. In a clear medium, diffusive mass fluxes relate to the concentration gradient. For low solute concentrations (*dilute* solution), the relationship is linear with the proportionality constant being given by the mass diffusivity of the solute in the solution. This treatment is quite similar to the heat flux—temperature gradient relationship contained in Fourier's law of heat conduction. In the mass transfer context, the linear relation, namely Fick's law, is written as

$$\dot{m}'' = -D\nabla C \tag{2.58}$$

Equation 2.58 connects mass flux (units of kg/m^2-s) and the concentration gradient via the mass diffusivity, D (units of m^2/s). Mass units can be equivalently expressed in molar form.

Consider mass transfer of a dissolved species in a flowing fluid. The physical law that governs the transport of the solute is the conservation of mass. In a clear medium, it leads to a mathematical form that is similar to thermal energy transport [59, 60] and is given as follows:

$$\left(\frac{\partial C}{\partial t} + \mathbf{u} \cdot \nabla C\right) = \nabla \cdot D \nabla C$$

In dilute solutions, diffusivity is practically independent of concentration, and the right-hand side can be expressed as $D\nabla^2 C$.

When the solutal mass balance equation is extended to a porous medium, mass diffusivity is replaced by the mass dispersion tensor D_m as in Eq. 2.32. Hence, for a porous medium

$$\left(\frac{\partial C}{\partial t} + \frac{\mathbf{u}}{\varepsilon} \cdot \nabla C\right) = \nabla \cdot [D_m] \nabla C \tag{2.59}$$

Here, $\mathbf{u}$ is Darcian velocity. Equation 2.59 assumes that solute transfer is in the liquid phase, with the solid media playing merely a passive role of creating tortuosity in the flow path. In this respect, Eq. 2.59 is analogous to the thermal equilibrium model discussed in Sect. 2.5.

Non-equilibrium effects as in Sect. 2.5.1 can appear in mass transfer if the solute precipitates out of the solution and deposits over the solid surface or is *adsorbed* by it. As a result, the solute fraction in the solution progressively diminishes in the flow direction. In many instances, the interest is in the solute concentration entirely in the fluid phase. The redistribution of salt within the solid particles may not be as relevant. In any case, mass transfer rates of salts in a solid phase are exceptionally slow, and the salt may be taken to reside entirely at the surface. The role of the solid phase in mass transfer is then to introduce purely a source term in Eq. 2.59. If the solid phase is assumed to remain clean at all times, the source term in the mass balance equation will be proportional to the local solute concentration. Hence, for a solute getting adsorbed into the solid phase

$$\left(\frac{\partial C}{\partial t} + \frac{\mathbf{u}}{\varepsilon} \cdot \nabla C\right) = \nabla \cdot [D_m] \nabla C - \beta C \tag{2.60}$$

The adsorption and dispersion parameters β and D_m have to be estimated independently from experiments. The adsorption parameter β may be estimated from reaction chemistry under certain circumstances.

If a model for the transport of solid phase concentration C^s is available, Eq. 2.60 can be rewritten for the solute concentration in the fluid phase $\left(C^f\right)$ as

$$\left(\frac{\partial C^f}{\partial t} + \frac{\mathbf{u}}{\varepsilon} \cdot \nabla C^f\right) = \nabla \cdot [D_m] \nabla C^f - \beta (C^f - C^s) \tag{2.61}$$

Equation 2.61 includes the following special cases:

(a) mass transfer of the solute from the solution to a clean matrix ($C^s = 0$ everywhere);

(b) mass transfer from a contaminated matrix to a clean solution ($C^s = 0$ on the inflow plane); apart from
(c) the general adsorption–desorption problem of contaminant transport in a porous medium.

Initial and boundary conditions for Eqs. 2.60 and 2.61 will depend on the physical problem being studied. For example, a salt solution entering a water-saturated porous medium will be subject to the following conditions:

$$\begin{aligned} &t = 0 \quad C^f(x,t) = 0\, C^s(x,t) = 0 \quad x > 0 \\ &x = 0 \quad C^f(x,t) = C_0^f C^s(x,t) = 0\, t > 0 \\ &x \to \infty \quad C^f(x,t) = 0\, C^s(x,t) = 0\, t > 0 \end{aligned} \tag{2.62}$$

Revised forms of Eq. 2.61 can be further developed for the following situations:

i. The transported species is radioactive with a decay constant d_λ. Here, the adsorption parameter β in Eq. 2.60 is replaced by $\beta + d_\lambda$.
ii. Species concentration is large, the dilute solution approximation is not valid, and diffusivity is a function of concentration.
iii. Dispersion models analogous to Eq. 2.32 are introduced.
iv. The incoming solution and the porous medium are at distinct temperatures, leading to a combined heat and mass transfer problem.
v. *Gas phase*: When gas (such as methane) is adsorbed on to the surface of the particles (of coal), the extent of adsorption depends on the local gas pressure. Thus, the adsorption–desorption process is determined by the difference in pressures between the gas phase and in the pores. For a gaseous medium, concentration can be related to pressure using the ideal gas law. With a and b as material-specific parameters, the concentration–pressure relation is given by the Langmuir equation

$$C = \frac{ap}{p+b}$$

2.8 Combined Heat and Mass Transfer

In a class of applications related to drying of an initially wet porous region, temperature gradients are jointly present with gradients of moisture content. Moisture here is present in the pore space in liquid form. With the bulk velocity taken to be zero, the mass flow rate and momentum equations need not be separately considered. The porous medium is taken to be homogeneous and isotropic for the present discussion, gravity effects are neglected, and the local thermal equilibrium model is

employed. Humidity is analogous to solute concentration considered in Sect. 2.7. The respective heat and mass fluxes are modified forms of the Fourier and Fick's laws of diffusion for heat and moisture migration and are given as

$$\begin{aligned} \dot{q}'' &= -k_m \nabla T \\ \dot{m}'' &= -D_m \nabla H - D_T \nabla T \end{aligned} \tag{2.63}$$

The model parameters of Eq. 2.63 are positive and are to be determined from experiments. Symbol D_T stands for the diffusion coefficient of mass transfer arising from a temperature gradient while k_m and D_m are the usual heat and mass transfer conductivity/diffusivity, respectively. For small evaporation rates from the liquid phase, Chang and Weng [61] have shown that these can be determined from principles of thermodynamics; also see [62].

The heat and mass transfer equations now solve for temperature (T) and moisture content (H) in the pore space and are given as:

$$\begin{aligned} (\rho C)_m \frac{\partial T}{\partial t} &= k_m \nabla^2 T + Q \\ \frac{\partial H}{\partial t} &= D_m \nabla^2 H + M \end{aligned} \tag{2.64}$$

Here, suffix 'm' refers to the effective medium properties of the porous region. Source terms Q and M refer to heat transfer arising from moisture migration primarily related to latent heat release and mass transfer related to possible condensation as well as the superimposed temperature gradient.

In the physical model, the solid phase, for example, wet sand dries during flow of dry air over it, changing its moisture and energy content. Thus, the energy source term can be written as

$$Q = (\rho h_{lv})_m \frac{\partial H}{\partial t}$$

Here, h_{lv} is the latent heat of evaporation of moisture at the local medium temperature. The mass source term in the moisture content equation is the divergence of mass flux associated with the temperature gradient and is expressed in one-dimensional form as

$$M = \frac{\partial}{\partial x}\left(D_T \frac{\partial T}{\partial x}\right)$$

Equation 2.64 is a coupled system of partial differential equations in terms of moisture content and temperature and can be numerically solved, subjected to suitable initial and boundary conditions.

Consider an initially wet, cold, horizontal, one-dimensional porous bed that is subjected to a temperature difference. Hence, the initial condition is:

$$t = 0 \quad T(y,t) = T_C; \quad H(y,t) = 1$$

The thermal boundary conditions are:

$$T(y = 0, t) = T_C; \quad T(y = L, t) = T_H$$

In many contexts, the lower surface is cooler to prevent natural convection effects.

The top surface is exposed to dry air from where water evaporates at a rate depending on the local mass transfer coefficient (h_m). Hence

$$-D_m \left.\frac{\partial H}{\partial y}\right|_{y=L} = h_m(H(L,t) - 1)$$

Assuming the lower boundary to be impermeable, the mass flux here is zero, leading to:

$$-D_m \left.\frac{\partial H}{\partial y}\right|_{y=0} - D_T \left.\frac{\partial T}{\partial y}\right|_{y=0} = 0$$

For large evaporation rates, the local pressure field is disturbed and a Darcian velocity component is to be added to the mass transfer equation. For a discussion on the drying of a porous medium using high temperature steam, see [63].

The above formulation can be extended to a porous medium filled with moist air and subjected to a cold boundary condition on one side. Under suitable conditions, water will condense on the cold side where it is drained, and the sign of vapor transport is reversed from the hot side toward the cold.

2.9 Flow, Heat, and Mass Transfer

In several applications, flow may arise from density differences in the fluid region, density being a function of temperature and species concentration. An example of such an application, shown in Fig. 2.7, is freshwater overlaid on saltwater, the overall arrangement subjected to a temperature difference [64–66]. Terms such as double-diffusive and triple-diffusive convection are often used in this context. For the present discussion, a thermal equilibrium model is adopted for heat transfer. The solid phase of the porous region is taken to be non-participating in mass transfer, solutal concentration referring to the fluid phase alone. The variation of fluid density with temperature and concentration can be assumed linear (within limits, [67]) and expressed as

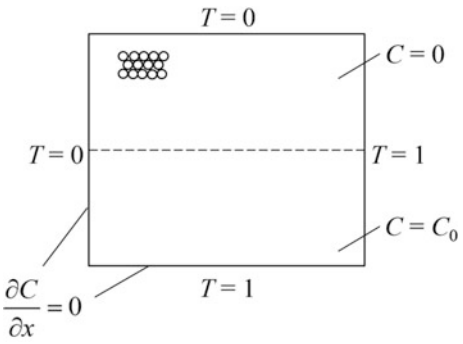

Fig. 2.7 An example where fluid flow is coupled with heat and mass transfer in a porous region. The walls are taken to be impermeable to mass transfer (mass flux = 0) while temperatures are prescribed

$$\rho = \rho_0(1 - \beta(T - T_0) + \gamma(C - C_0))$$

Here, suffix '0' indicates a reference state, for example, the initial undisturbed condition of the fluid region. Symbols β and γ refer to the volumetric expansion coefficient of the fluid relative to temperature (positive, K^{-1}) and concentration (positive, $(mg/l)^{-1}$), respectively. It is expected that an increase in temperature will lower density while increase in concentration will increase density further. Hence, coefficients β and γ are expected to be positive quantities. Body force contributions arise from distortions in temperature and concentration that perturb the density field. Changes in density and other fluid properties are neglected in other terms, for example, inertia and viscous. Such an approach is called the *Boussinesq* approximation [67].

With z as a coordinate oriented in the vertical direction, we define a modified pressure for ease of mathematical formulation as follows:

$$\tilde{p} = p + \rho_0 g z$$

The mass, momentum, energy, and solutal transport equations can be jointly written as:

$$\begin{aligned}
\nabla \cdot \mathbf{u} &= 0 \\
\frac{\rho_0}{\varepsilon}\left(\frac{\partial \mathbf{u}}{\partial t} + \frac{\mathbf{u}}{\varepsilon} \cdot \nabla \mathbf{u}\right) &= -\nabla \tilde{p} + \rho_0 g[\beta(T - T_0) - \gamma(C - C_0)]\mathbf{k} - \frac{\mu}{K}\mathbf{u} \\
&\quad - \frac{\rho F}{\sqrt{K}}\mathbf{u}^2 + \frac{\mu}{\varepsilon}\nabla^2 \mathbf{u} \\
(\rho C)_m \frac{\partial T}{\partial t} + (\rho C)_f \mathbf{u} \cdot \nabla T &= \nabla \cdot [k_m]\nabla T \\
\left(\frac{\partial C}{\partial t} + \frac{\mathbf{u}}{\varepsilon} \cdot \nabla C\right) &= \nabla \cdot [D_m]\nabla C
\end{aligned} \tag{2.65}$$

In Eq. 2.65, **k** is a unit vector in the vertically upward direction. Note that temperature and concentration effects are opposed to each other in the sense that concentration variation as in Fig. 2.7 can diminish velocities and stabilize the flow field.

For the problem shown in Fig. 2.7, the initial and boundary conditions are:

$$t = 0\, \mathbf{u} = 0,\ T = 0,\ C = F(z)$$
$$\text{walls}, \mathbf{u} = 0, T = \text{given}, \frac{\partial C}{\partial n} = 0$$

Here, n is the outward drawn normal on a solid surface. In Eq. 2.65, flow is set up due to inhomogeneities in the density field arising from a distribution of solutal concentration and temperature. In this respect, the system of equations in (2.65) is coupled and needs to be jointly solved.

2.10 Nanoscale Porous Media

Hydrocarbons (liquids as well as gases), water, and aqueous solutions can occupy pores and fractures of natural reservoirs whose length scales extend from a few millimeters down to nanometers. Pores in membranes used for distillation and component separation are in the nanometer range. The overall characteristics of the flow and transport processes depend on the connectivity of the pores over the length scales, and the details of the physical processes, as one proceeds from the macro- to the micropores in the porous medium. If there were to be no change in the physical laws underlying transport of mass, momentum, and energy, it would be appropriate to define effective properties for quantities such as permeability, conductivity, and dispersion and treat the porous region as a continuum. This assumption has been implicitly utilized in analysis when length scales varied over two or three orders of magnitude. The issue of whether it holds over a spread of 6–7 orders of magnitudes is as yet unresolved. Preliminary research shows that significant differences are to be anticipated. For example, small pore dimensions in the micron range will yield effective permeability greater than what is predicted by Eq. 1.3.

The flow of fluids, fluid–matrix interactions, chemical reactions, and wetting characteristics in a nano-environment are topics of research that have just begun to be reported in the literature [68–72]. It calls for molecular level experiments as well as simulation to relate microscopic concepts of surface texture, three-phase contact line, and probability distribution functions to the macroscopic, such as temperature and pressure. The determination of effective medium properties in the presence of nanoscale phenomena is the next challenge in the study of transport phenomena in porous media.

2.11 Multiscale Porous Media

The heterogeneity of a porous medium can be accounted for in the mathematical model by treating quantities such as permeability and dispersion coefficient as space-dependent model parameters that are determined from carefully calibrated inverse experiments. Meaningful predictions are possible when permeability variations are continuous and within limits. This approach is, however, unsatisfactory from a theoretical viewpoint, when the degree of heterogeneity is quite high. This is because the model parameters thus determined are likely to be specific to the application considered; in addition, they could be scale- and phenomenon-dependent as well.

A greater generality can be built into the theory of transport phenomena in porous media, by assigning a mathematical structure to the heterogeneity of the physical region. The fractal structure is an example, wherein the pore scales have a continuous variation in the wave number space and equivalently show an infinite correlation length in the physical space [73, 74]. The macroscopic properties now depend on the fractal dimensions, along with adjustable coefficients that are to be determined from experiments.

The pore geometry of heterogeneous porous media may not have a fractal structure but can show a hierarchical variation in many applications. As described by Cushman and coworkers [75–77], this indicates that the macroscopic medium can be decomposed into successively nested, interacting physical subunits. The decomposition can be discrete or continuous; the available literature has examined a finite number of hierarchies in the porous region. It is possible for the physical phenomena at every ladder of the hierarchy to be identical, except that they develop inter-dependence at their interfaces. Alternatively, the physical dimensions may be so far apart that transport processes in the hierarchy are quite distinct. For example, it is conceivable that the smallest length scales fall in the micro- or the nanorange, while the bulk of the porous region is at the macroscale. This is an example of functional hierarchy in transport processes coexisting with the structural hierarchy of the porous region. For a discussion on transport in a two-level hierarchy, dual porosity system, see [78].

The differences in the volume-averaged governing equations between homogeneous and hierarchical porous media become clear from the following discussion. A scalar function is denoted as $F(x)$ in the space variable x while $\mathbf{F}(x)$ is a vector-valued function. For a homogeneous region, Gauss divergence theorem can be written for the scalar- and vector-valued functions, respectively, as follows:

$$\begin{aligned} \int_{\omega} \nabla F(x) dV &= \int_{\partial\omega} F(x) n dS \\ \int_{\omega} \nabla \cdot \mathbf{F}(x) dV &= \int_{\partial\omega} \mathbf{F}(x) \cdot n dS \end{aligned} \tag{2.66}$$

Here, ω is a representative volume, and $\partial\omega$ is its surface, with n being a unit outward drawn normal on the surface. When the above relations are applied to a heterogeneous medium, volume ω is replaced by ω_1, the volume occupied by all particles and pores at scale 1 (the corresponding hierarchy). In addition, $\partial\omega_1$ is the partial surface area at this scale, and $\partial\omega$ is the total surface area. Gauss's theorem applied to a single scale of the hierarchy can be derived as [79]:

$$\begin{aligned}\int_{\omega} \nabla F(x)dV &= \nabla \int_{\omega_1} F(x)dV + \int_{\partial\omega-\partial\omega_1} F(x)ndS \\ \int_{\omega} \nabla\cdot\mathbf{F}(x)dV &= \nabla\cdot \int_{\omega_1} \mathbf{F}(x)dV + \int_{\partial\omega-\partial\omega_1} \mathbf{F}(x)\cdot ndS\end{aligned} \tag{2.67}$$

The additional terms in the above equations (relative to Eq. 2.66) significantly increase the mathematical complexity of the governing equations.

The process of integrating the governing equations over a subdomain of the physical space can give rise to constitutive variables that have a *non-local* character. It will require parameter estimation experiments to be conducted at appropriate scales, and not the macroscale alone. These are additional complications in the study of flow and transport in hierarchical porous media.

Vankan et al. [80] derived equations for blood perfusion in a biological tissue using the hierarchical mixture theory. While blood is the fluid of interest, the pores in the tissue form on the lowest scale of the porous medium. At a larger length scale, a few larger arteries supply blood through a diverging, arteriolar vascular channel. Blood reaches the capillaries and is subsequently drained by the converging veins. Blood vessels are numerous, uniformly distributed, and occupy a large part of the hierarchy. Geometric and mechanical properties of the vascular structure such as diameter, wall thickness and stiffness, orientation and density depend on the hierarchy being addressed. Consequently, the flow field is a function of position on one hand and exhibits on the other, a dependence on the scale at which the flow takes place.

The mathematical formulation for transport of heat and moisture in an unsaturated porous medium with three spatial scales is developed in [77]. It is shown here that the number of variables that need to be specified via constitutive relationships is over 30! Thus, a general formulation of transport in continuous hierarchical porous media has considerable challenge.

2.12 Closure

Derivation of equations governing flow, heat, and mass transfer in porous media is discussed in the present chapter. The starting point is Darcy's law that can be gradually extended to higher flow rates, complex pore geometries, and the

appearance of interfaces of immiscible fluids. A second starting point is the system of equations valid for a homogeneous fluid medium; it can be generalized to a multiphase system such as a porous medium by introducing source terms and effective medium properties. In each approach, the model carries a large number of parameters that are sensitive to the pore structure, though to a lesser extent on the thermophysical properties of the constituent media. Thus, success in modeling transport in porous media is linked to careful parameter estimation from experiments. This step is expected to become critical in multiscale porous media where the pore scales span several orders of magnitude. Theoretical derivation of the applicable form of the governing equations may prove to be advantageous under these circumstances. Modeling flow in the non-continuum regime is discussed in Chap. 3.

References

1. J. Bear, *Dynamics of Fluids in Porous Media* (American Elsevier Pub. Co., New York, 1972)
2. J. Bear, Y. Bachmat, *Introduction to Modeling of Transport Phenomena in Porous Media* (Kluwer, Dordrecht, 1990)
3. S. Whitaker, *The Method of*, vol. Averaging (Kluwer Academic Publishers, Boston, 1999)
4. G.F. Pinder, *Essentials of Multiphase Flow and Transport in Porous Media* (Wiley, Hoboken, 2008)
5. M. Kaviany, *Principles of Heat Transfer in Porous Media* (Mechanical Engineering Series, Springer, New York, 1991)
6. K. Vafai (ed.), *Handbook of Porous Media*, 3rd edn. (CRC Press, Boca Raton, USA, 2015)
7. J. Bear, A. Verruijt, *Modeling Groundwater Flow and Pollution* (Reidel, Dordrecht, 1987)
8. D.B. Ingham, I. Pop, *Transport Phenomena in Porous Media* (Pergamon Press, Oxford, 2002)
9. D.A. Nield, A. Bejan, *Convection in Porous Media*, 4th edn. (Springer, New York, 2013)
10. M. Le Ravaled-dupin, *Inverse Stochastic Modeling of Flow in Porous Media* (Technip, Paris, 2005)
11. F. White, *Fluid Mechanics*, 2nd edn. (McGraw-Hill, New York, 1986)
12. F.W. Schwartz, H. Zhang, *Fundamentals of Groundwater* (Wiley, New York, 2003)
13. C.R. Fitts, *Groundwater Science* (Academic Press, London, 2002)
14. D.W. Hahn, M.N. Ozisik, *Heat Conduction*, 3rd edn. (Wiley, New Jersey, 2012)
15. M. Sahimi, *Flow and Transport in Porous Media and Fractured Rock* (Wiley, New Jersey, 2011)
16. A. Amiri, K. Vafai, Analysis of dispersion effects and non-thermal equilibrium, non-Darcian, variable porosity incompressible flow through porous media. Int. J. Heat. Mass Transf. **37**, 939–954 (1994)
17. M. Sozen, T.M. Kuzay, Enhanced heat transfer in round tubes with porous inserts. Int. J. Heat Fluid Flow **17**, 124–129 (1996)
18. A.V. Kuznetsov, K. Vafai, Analytical comparison and criteria for heat and mass transfer models in metal hydride packed beds. Int. J. Heat Mass Transf. **38**, 2873–2884 (1995)
19. C.A.J. Fletcher, Computational Techniques for Fluid Dynamics, Vol. I and II, Springer, New York, 1988
20. J.D. Anderson Jr., *Modern Compressible Flow with Historical Perspective* (McGraw-Hill, New York, 1990)

21. P.G. Drazin, W.H. Reid, *Hydrodynamic Stability* (Cambridge University Press, Cambridge, UK, 1981)
22. M.J.S. de Lemos, M.H.J. Pedras, Recent mathematical models for turbulent flow in saturated rigid porous media. ASME Fluids Engg. **123**(4), 935–940 (2001)
23. Y. Takatsu, T. Masuoka, Turbulent phenomena in flow through porous media. J. Porous Media **1**, 243–251 (1998)
24. M.J.S. de Lemos, *Turbulent Impinging Jets into Porous Materials* (Springer Briefs in Computational Mechanics, New York, 2012)
25. P. Holmes, J.J. Lumley, G. Berkooz, C.W. Rowley, *Turbulence, Coherent Structures, Dynamical Systems, and Symmetry* (Cambridge University Press, Cambridge, 2012)
26. H. Schlichting, Boundary-layer Theory, McGraw-Hill, New York, 1979 (8th edition: 2000)
27. D. Getachew, W.J. Minkowycz, and J.L. Lage, A modified form of the k-ε model for turbulent flow of an incompressible fluid in porous media. Int. J. Heat Mass Transfer, pp. 2909–2915, 2000
28. W.M. Kays, M.E. Crawford, *Convective Heat and Mass Transfer*, 3rd edn. (McGraw-Hill, New York, 1993)
29. S.M. Ghiaasiaan, *Convective Heat and Mass Transfer* (Cambridge University Press, Cambridge, 2011)
30. L.C. Davis, B.E. Artz, Thermal conductivity of metal-matrix composites. J. Appl. Phys. **77** (10), 4954–4958 (1995)
31. G. Degan, *Flow and Transport in Porous Formations* (Springer-Verlag, Berlin, 1989)
32. C.T. Hsu, P. Cheng, Thermal dispersion in a porous medium. Int. J. Heat Mass Transf. **33**, 1587–1598 (1990)
33. A. Levy, S. Sorek, G. Ben-Dor, J. Bear, Evolution of the Balance Equations in Saturated Thermoelastic Porous Media following abrupt simultaneous changes in Pressure and Temperature. Transp. Porous Media **21**, 241–268 (1998)
34. A. Levy, G. Ben-Dor, S. Sorek, Numerical Investigation of the Propagation of Shock waves in Rigid Porous Materials: Flow Field Behaviour and Parametric Study. Shock Waves **8**, 127–137 (1998)
35. A. Hunt, R. Ewing, *Percolation Theory for Flow in Porous Media* (Springer, Berlin, 2009)
36. C.M. Case, *Physical Principles of Flow in Unsaturated Porous Media* (Oxford University Press, Oxford, 1994)
37. MTh van Genuchten, A Closed-Form Equation for Predicting the Hydraulic Conductivity of Unsaturated Soils. Soil Sci. Soc. Am. J. **44**(5), 892–898 (1980)
38. A. Szymkiewicz, *Modelling Water Flow in Unsaturated Porous Media* (Springer, New York, 2013)
39. T.C. Boberg, *Thermal Methods of Oil Recovery: An Exxon Monograph* (Wiley, New York, 1988)
40. R.E. Ewing, *The Mathematics of Reservoir Simulation* (SIAM, Philadelphia, 1983)
41. P. Daripa, J. Glimm, B. Lindquist, M. Maesumi, O. McBryan, On the simulation of heterogeneous petroleum reservoirs, in *Numerical Simulation in Oil recovery*, vol. 11, ed. by M.F. Wheeler, The IMA Volume in Mathematics and its Applications, (Springer-Verlag, 1986), pp 89–103
42. K. Aziz, Modeling of thermal oil recovery processes, in *Mathematical and Computational Methods in Seismic Exploration and Reservoir Modeling*, ed. by W.E. Fitzgibbon (Philadelphia, SIAM, 1986), pp. 3–17
43. D.S. Oliver, Multiple realizations of the permeability field from well-test data. Soc. Petrol. Eng. J. **1**(2), 145–154 (1996)
44. A.C. Reynolds, N. He, L. Chu, D.S. Oliver, Reparameterization techniques for generating reservoir descriptions conditioned to variograms and well-test pressure data. Soc. Petrol. Eng. J. **1**(4), 413–426 (1996)
45. F. Zhang, A.C. Reynolds, D.S. Oliver, Evaluation of the reduction in uncertainty obtained by conditioning a 3D stochastic channel to multiwell pressure data. Math. Geol. **34**(6), 715–742 (2002)

46. F. Civan, Implications of alternate macroscopic descriptions illustrated by general balance and continuity equations. J. Porous Media **5**(4), 271–282 (2002)
47. P.K.W. Vinsome, Fully implicit versus dynamic implicit reservoir simulation. J. Canadian Petro. Tech., 49–82, 1985
48. R. Lenormand, E. Touboul, C. Zarcone, Numerical models and experiments on immiscible displacements in porous media. J. Fluid Mech. **189**, 165–187 (1988)
49. C.T. Tan, G.M. Homsy, Simulation of nonlinear viscous fingering in miscible displacement. Phys. Fluids **31**(6), 1330–1338 (1988)
50. M.D. Stevenson, M. Kagan, W.V. Pinczewski, Computational methods in petroleum reservoir simulation. Comput. Fluids **19**, 1–19 (1991)
51. H.R. Zhang, K.S. Sorbie, N.B. Tsibuklis, Viscous fingering in five-spot experimental porous media: new experimental results and numerical simulation. Chem. Eng. Sci. **52**, 37–54 (1997)
52. G. Ahmadi, C. Ji, D.H. Smith, Numerical solution for natural gas production from methane hydrate dissociation. J. Petrol. Sci. Eng. **41**, 269–285 (2004)
53. G.C. Fitzgerald, M.J. Castaldi, Y. Zhou, Large scale reactor details and results for the formation and decomposition of methane hydrates via thermal stimulation dissociation. J. Petrol. Sci. Eng. **94**, 19–27 (2012)
54. G.J. Moridis, T.S. Collett, R. Boswell, M. Kurihara, M.T. Reagan, C.A. Koh, Toward production from gas hydrates: current status, assesment of resources, and simulation-based evaluation of technology and potential. SPE Reserv Eval. Eng. **12**(5), 745–771 (2009)
55. E.D. Sloan Jr., C.A. Koh, Clathrate Hydrates of Natural Gases 3rd Edition, Series: Chemical Industries, Vol. 119, CRC Press, 2007
56. M. Uddin, D.A. Coombe, D. Law, W.D. Gunter, Numerical studies of gas hydrate formation and decomposition in a geological reservoir. ASME J Energy Resour Technol. **130**(3), 10–17 (2008)
57. M.D. White, S.K. Wurstner, B.P. McGrail, Numerical studies of methane production from class 1 gas hydrate accumulations enhanced with carbon dioxide injection. Mar. Pet. Geol. **28** (2), 546–560 (2011)
58. F. Civan, *Porous Media Transport Phenomena* (Wiley, New Jersey, 2011)
59. D. Ingham, A. Bejan, E. Mamut, I. Pop (eds.), *Emerging Technologies and Techniques in Porous Media* (Springer, New York, 2012)
60. J.M.P.Q. Delgado (ed.), *Heat and Mass Transfer in Porous Media* (Springer, New York, 2012)
61. W.J. Chang, C.I. Weng, An Analytical Solution to Coupled Heat and Moisture Diffusion Transfer in Porous Materials. Int. J. Heat Mass Transf. **43**, 3621–3632 (2000)
62. K.K. Khankari, R.V. Morey, S.V. Patankar, Mathematical Model for Moisture Diffusion in Stored Grain due to Temperature Gradients, Transactions of ASME –. J. Heat Transf. **37**(5), 1591–1604 (1994)
63. P. Perre, M. Moser, M. Martin, Advances in Transport Phenomena during Convective Drying with Superheated Steam and Moist Air. Int. J. Heat Mass Transfer **36**(1), 2725–2746 (1993)
64. A. Mojtabi, M.C. Charrier-Mojtabi, Double diffusive convection in porous media, in *Handbook of Porous Media*, ed. by K. Vafai (Taylor and Francis, New York, 2005), pp. 269–320
65. A.V. Kuznetsov, D.A. Nield, The Cheng-Minkowycz problem for the double-diffusive natural convective boundary layer flow in a porous medium saturated by a nanofluid. Int. J. Heat Mass Transf. **54**, 374–378 (2011)
66. S. Rionero, Triple diffusive convection in porous media. Acta Mech. **224**, 447–458 (2013)
67. B. Gebhart, Y. Jaluria, R.L. Mahajan, B. Sammakia, *Buoyancy-Induced Flows and Transport* (Springer, New York, 1988)
68. S. Roy, R. Raju, H.F. Chuang, B.A. Crudent, M. Meyyappan, Modeling gas flow through microchannels and nanopores. J. Appl. Phys. **93**(8), 4870–4879 (2003)
69. V.P. Sokhan, D. Nicholson, N. Quirke, Fluid flow in nanopores: an examination of hydrodynamic boundary conditions. J. Chem. Phys. **115**(8), 3878–3887 (2001)

70. M. Gad-el-Hak, The fluid mechanics of microdevices—The Freeman Scholar lecture. ASME J. Fluids Eng. **121**, 6–33 (1999)
71. G.A. Bird, *Molecular Gas Dynamics and the Direct Simulation of Gas Flows* (Clarendon Press, Oxford, 1994)
72. G. Karniadakis, A. Beskok, *Micro Flows-Fundamentals and Simulation* (Springer, New York, 2002)
73. R. Pitchumani, B. Ramakrishnan, A fractal geometry model for evaluating permeabilities of porous performs used in liquid composite molding. Int. J. Heat Mass Trans. **42**, 2219–2232 (1999)
74. S.W. Wheatcraft, G.A. Sharp, S.W. Tyler, Fluid flow and transport in fractal heterogeneous porous media, Chapter XI in *Dynamics of Fluids in Hierarchical Porous Media*, ed. By J.H. Cushman, Academic Press, New York, 1990
75. J.H. Cushman (ed.), *Dynamics of Fluids in Hierarchical Porous Media* (Academic Press, New York, 1990)
76. J.H. Cushman, *The Physics of Fluids in Hierarchical Porous Media: Angstroms to Miles* (Kluwer Academic, Dordrecht-Boston, 1997)
77. L.S. Bennethum, J.H. Cushman, Coupled solvent and heat transport of a mixture of swelling porous particles and fluids: single time-scale problem. Transp. Porous Media **36**, 211–244 (1999)
78. C.Y. Wang, C. Beckermann, Single vs. dual-scale volume averaging for heterogeneous multiphase systems. Int. J. Multiphase Flow **19**(2), 397–407 (1993)
79. V.S. Travkin, I. Catton, Transport phenomena in heterogeneous media based on volume averaging theory. Adv. Heat Transf. **34**, 1–144 (2001)
80. W.J. Vankan, J.M. Huyghe, M.R. Drost, J.D. Janssen, A. Huson, A finite element mixture model for hierarchical porous media. Int. J. Numer. Meth. Engg. **40**, 193–210 (1997)

http://www.springer.com/978-3-319-69864-9

Modeling Transport Phenomena in Porous Media with Applications

Das, M.K.; Mukherjee, P.P.; Muralidhar, K.

2018, XI, 241 p. 76 illus., 51 illus. in color., Hardcover
ISBN: 978-3-319-69864-9